Chapter 12

VARIATIONS OF GALACTIC COSMIC RAYS AND THE EARTH'S CLIMATE

Jasper Kirkby
CERN
Geneva 23, Switzerland
jasper.kirkby@cern.ch

Kenneth S. Carslaw
University of Leeds, School of Earth & Environment
Leeds LS2 9JT, United Kingdom
carslaw@env.leeds.ac.uk

Abstract The galactic environment of Earth appears to have varied only subtly over mankind's time scale. Have these variations had any perceptible effect on Earth's climate? Surprisingly, they may; palaeoclimatic evidence suggests that the climate may be influenced by solar/cosmic ray forcing on all time scales from decades to billions of years. However, despite an intense scientific interest spanning two centuries, the mechanism underlying solar-climate variability has remained a mystery. Recent satellite data, however, have provided an intriguing new clue: low cloud cover may be influenced by galactic cosmic rays. Since cosmic rays are modulated by the solar wind, this would link Earth's climate to solar *magnetic* activity, which is known to be highly variable. On longer time scales, it would also imply that the climate responds to changes in the geomagnetic field and the galactic environment of Earth, both of which affect the cosmic ray flux. The least understood aspect of this sequence of processes is the microphysical mechanism by which cosmic rays may affect clouds. Physical mechanisms have been proposed and modelled, but definitive experiments are lacking. However, the presence of ion-induced nucleation of new particles in the atmosphere is supported by recent observations, and new experiments are underway to investigate the nature and significance of cosmic ray-cloud-climate interactions.

P. C. Frisch (ed.), Solar Journey: The Significance of our Galactic Environment for the Heliosphere and Earth, 349–397.

Keywords: Solar-cosmic ray-climate variability, solar irradiance, galactic cosmic rays, palaeoclimate, cosmic ray-cloud-climate mechanisms, ion-induced nucleation, ice nucleation, global electric circuit

1. Introduction

The first observation of solar-climate variability was recorded two centuries ago by the astronomer William Herschel [Herschel, 1801] who noticed that the price of wheat in England was lower when there were many sunspots, and higher when there were few. The most well-known example of a solar-climate effect is known as the Maunder Minimum [Eddy, 1976], the period between 1645 and 1715—which ironically coincides with the reign of Louis XIV, *le Roi Soleil*, 1643–1715—during which there was an almost complete absence of sunspots (Fig. 12.1). This marked the most pronounced of several prolonged cold spells in the period between about 1450 and 1850 which are collectively known as the Little Ice Age. During this period the River Thames in London regularly froze across, and fairs complete with swings, sideshows and food stalls were a standard winter feature. Numerous studies of palaeoclimatic proxies have both confirmed that the Little Ice Age was a global phenomenon and, moreover, that it was but one of around 10 occasions during the Holocene when the Sun entered a grand minimum for a centennial-scale period, and Earth's climate cooled (§4.3.0).

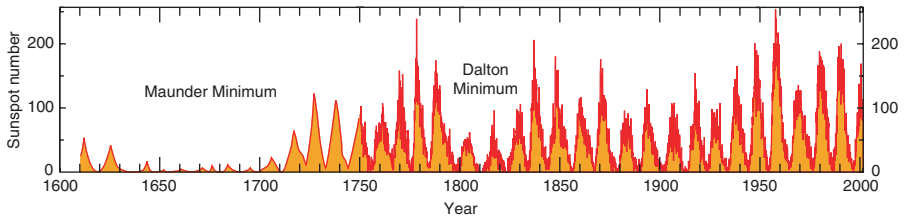

Figure 12.1. Variation of the sunspot number from 1610 to 2001. The record starts 3 years after the invention of the telescope by Lippershey in Holland.

However, despite the widespread evidence, solar variability remains controversial as a source of climate change since no causal mechanism has been established to link the two phenomena. The most obvious mechanism to consider would be the possibility of a variable solar irradiance, but estimates of long-term irradiance changes based on sun-like stars appear to be insufficient to cause the observed climate variations (§2.2.0). The physical mechanism for solar-climate variability therefore remains a mystery.

However, an important new clue has recently been provided by satellite data which reveal a surprising correlation between galactic cosmic

ray (GCR) intensity and the fraction of Earth covered by low clouds [Svensmark and Friis-Christensen, 1997, Marsh and Svensmark, 2003]. Since changes of solar magnetic activity affect the solar wind and thereby modulate the GCR intensity, this could provide the long-sought missing link between solar- and climate variability. If more cosmic rays lead to more low clouds, this would exert a strong cooling influence on the radiative energy balance of Earth. It would explain how a tiny energy input from GCRs to the atmosphere—comparable to starlight—could produce such large changes in the climate. Clouds cover a large fraction of Earth's surface (a global annual mean of about 65%) and exert a strong net cooling effect of about 28 Wm^{-2}[Hartmann, 1993], so long-term variations of only a few per cent would be climatically significant.

Moreover, if this mechanism were to be established, it could have significant consequences for our understanding of the solar contribution to the present global warming. The globally-averaged GCR intensity declined by about 15% during the 20^{th} century due to an increase of the solar open magnetic flux by more than a factor of two [Lockwood *et al.*, 1999]. If the cosmic ray-cloud effect is real then the implied reduction of low cloud cover by about 1.3% absolute could have given rise to a radiative forcing of about $+0.8\mathrm{Wm}^{-2}$, which is comparable to the estimated total anthropogenic forcing of about $+1.3\ \mathrm{Wm}^{-2}$ [IPCC, 2001].

A GCR-cloud effect would provide an indirect mechanism to amplify solar forcing, bringing additional uncertainties to climate change projections. The Intergovernmental Panel on Climate Change (IPCC) stated in its Third Assessment Report (2001) that "mechanisms for the amplification of solar forcing are not well established". The solar amplification mechanism–which appears to drive the large centennial-scale climate variations seen, for example, in Fig. 12.8—is absent from present climate models. Since these natural climate variations are comparable to the present global warming, they must be properly accounted for before we can reliably interpret 20^{th} century climate change and confidently predict future warming due to anthropogenic greenhouse gases.

2. Solar Irradiance

2.1 Climate Sensitivity to Radiative Forcing

To interpret how Earth would respond to a radiative forcing, it is useful to consider the climate sensitivity. Climate models indicate an approximately linear relationship between global mean radiative forcing, Q (Wm^{-2}), and the equilibrium global mean surface temperature change, ΔT (K),

$$\Delta T = \lambda\, Q$$

where λ (K/Wm^{-2}) is the climate sensitivity parameter. This parameter is relatively insensitive to the nature of the forcing—for example, greenhouse gases or solar irradiance—provided the forcing agent is not highly variable spatially (like, for example, aerosols). All climate feedback processes, such as changes in water vapour, clouds or ice sheet albedo, are implicitly included in λ.

The value of λ can be inferred in several ways. Climate models indicate a doubling of the concentration of atmospheric CO_2 from pre-industrial levels (280 ppm) produces +4 Wm^{-2} forcing and a mean temperature rise ranging from 1.5 K to 4.5 K, with a central value of 3 K [IPCC, 2001]. Therefore $\lambda \simeq (3 \pm 1.5)/4 = (0.75 \pm 0.4)\,\mathrm{K/Wm^{-2}}$. This is consistent with the estimate, $\lambda \simeq 5$ K / 7 Wm^{-2} $= 0.7\,\mathrm{K/Wm^{-2}}$, obtained from ice core samples for the transition between glacial and interglacial periods. Using this value, the possible contribution of +0.8 Wm^{-2} from a cosmic ray-cloud effect during the 20^{th} century (§1) would translate to a temperature rise of around $0.7 \times 0.8 = 0.6$ K, which would be highly significant.

These figures can be compared with the response of Earth if it were simply to act as a black body. In this case the radiant emittance is $R = \sigma T^4$, where σ is the Stefan-Boltzmann constant. The radiation from a black body varies as $\Delta R/R = 4\Delta T/T$, so that $\Delta T = (T/4R)\,\Delta R$. Since $\Delta R/R = \Delta I/I$, the fractional change in solar irradiance, it follows that $\lambda_0 = T/4I$. The global mean solar irradiance reaching the lower troposphere is $I \simeq 0.7 \times 1366/4 \simeq 240\,\mathrm{Wm^{-2}}$ (the factor 0.7 accounts for shortwave albedo and the factor 4 averages the solar irradiance of 1366 Wm^{-2} over the full surface area of Earth). The effective radiating temperature of Earth is then given by $240 = \sigma T^4$, indicating $T = 255$ K. (This is the effective blackbody temperature of Earth as seen from a satellite, corresponding to radiation from the final scattering layer in the upper troposphere.) We thereby estimate $\lambda_0 = 255/(4 \cdot 240) = 0.26\,\mathrm{K/Wm^{-2}}$ for Earth in the absence of any feedbacks. Therefore Earth's climate feedback factor is about 2.5, which indicates the presence of positive feedbacks that amplify the response to a radiative forcing.

2.2 Solar Irradiance Variability

Solar cycle variability. Solar radiometry measurements made by satellites over the last 25 years have shown that the so-called solar constant varies by about 0.08% over the solar cycle (Fig. 12.2). Counter-intuitively, the Sun radiates more during periods of high solar magnetic activity since, although the sunspots are cooler than the mean temperature of the photosphere (around 5840 K), they are more than compensated by the associated bright *faculae*.

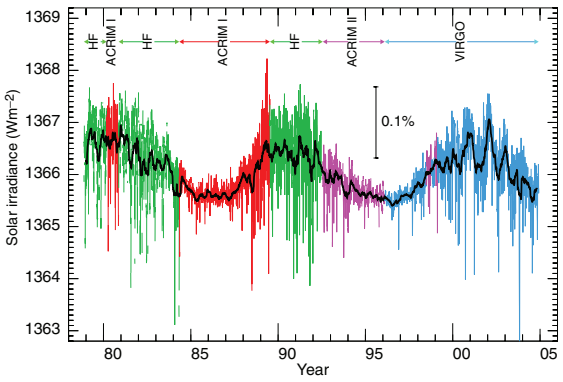

Figure 12.2. Total solar irradiance at the top of Earth's atmosphere over the last 2.5 solar cycles (updated from [Fröhlich, 2000]). The curve is a composite of several satellites, each covering a different time interval, as indicated by the different coloured regions of the curve and the labels shown above it. Peak irradiance corresponds to sunspot maximum (and GCR minimum). The large high-frequency fluctuations are due to sunspots rotating in and out of the field of view.

A variation of solar irradiance by 0.08% (1.1 Wm^{-2}) over the sunspot cycle corresponds to a global mean variation of $0.7 \times 1.1/4 = 0.2\,\mathrm{Wm}^{-2}$ at Earth's surface. This would be expected to produce an *equilibrium* temperature change $\Delta T = 0.7 \times 0.2 = 0.14$ K. However the large thermal inertia of the well-mixed upper 100 m layer of the oceans will reduce the actual temperature response. This damping effect can be estimated by considering an analogous electromagnetic RC-circuit equivalent for the ocean surface layer: a resistor and capacitor in series, which are set into forced oscillation by a sinusoidal voltage [Kirkby, 2002]. In this analogy, forcing heat fluxes are analogous to current, temperature to voltage, the ocean to a capacitor and the climate sensitivity parameter to a resistor. The estimated attenuation factors are large, e.g. a factor 5 for $\lambda = 0.7$ K/Wm^{-2}, corresponding to an 8.4 yr time constant and phase lag of about 80°. This implies the expected response of Earth's mean surface temperature to irradiance variability over the solar cycle is only about 0.03 K.

Although this is a challenging measurement, sea-surface temperature data over the last century do indeed reveal signals of the 11-yr solar cycle in the Indian, Pacific and Atlantic Oceans [White *et al.*, 1997, White *et al.*, 1998]. The solar cycle peak-to-peak amplitude is (0.06 ± 0.005) K and it lags the changes in solar irradiance by about 0–65°.

Secular Solar Variability. Irradiance variations over the 11-yr sunspot cycle are now well established and, moreover, reasonably well explained in terms of sunspot darkening and faculae brightening. However, the important question for climate is whether or not there are also underlying secular variations on longer time scales. Even a variation of comparable magnitude—0.1%—would be significant since the climate response would not be damped by the thermal inertia of the oceans.

The Lean *et al.* (1995) estimate of the long-term variation of solar irradiance has been widely used in climate models to calculate the solar contribution to climate change in the 20^{th} century [IPCC, 2001] and in the period since the Maunder Minimum. It is based on observations of luminosity variations in Sun-like stars and on a speculated long-term relationship between solar luminosity and solar magnetic activity. Cosmic ray flux, recorded in ^{10}Be concentrations in ice cores (§3.3), are used as a proxy for solar magnetic activity. The estimated secular increase of irradiance since 1700 is about 2.6 Wm^{-2}, with a superimposed variation of up to about 1 Wm^{-2} due to the sunspot cycle [Lean *et al.*, 1995]. This translates to a top-of-the-atmosphere long-term solar radiative forcing of $(0.7/4) \cdot 2.6 = 0.46$ Wm^{-2} (§2.1), corresponding to a temperature change of $0.7 \times 0.46 = 0.32$ K.

This figure may be compared with palaeoclimatic reconstructions, which suggest global temperatures were around 0.7 K cooler during the Maunder Minimum, after subtracting the estimated anthropogenic contributions during the last century (§4.2). The estimated irradiance variations therefore appear to be too small by about a factor two to account for the observed temperature change. Moreover, new results on Sun-like stars and new modelling studies have brought the Lean *et al.* (1995) estimate into question [Foukal *et al.*, 2004]. Indeed, the original authors have now accepted [Lean *et al.*, 2002] that their 1995 calculations of long-term irradiance variations may be over-estimated by about a factor five. This would imply a temperature change of only 0.06 K from solar irradiance variations since the Maunder Minimum, which would account for only a small fraction—about 10%—of the observed change.

The absence of evidence for long-term solar irradiance changes does not, of course, rule them out. It does, however, underscore how little is understood about the mechanism for solar-climate variability. Moreover, it implies that current general circulation model (GCM) simulations of 20^{th} century warming may substantially over-estimate the contribution from solar irradiance variability. The clear solar signal in the 20^{th} century temperature record (§4.1)—and also at earlier times—is therefore unexplained. A solar amplification mechanism could solve this puzzle.

3. Galactic Cosmic Rays

3.1 Solar-climate Mechanisms

There are only two physical paths that could connect variations of the Sun to Earth's climate: 1) solar electromagnetic radiation (either irradiance or else a spectral component such as the ultraviolet, UV), or 2) galactic cosmic rays, whose intensity is modulated by the solar wind. A direct interaction of the solar wind with the troposphere can probably be excluded since the charged particles of the solar wind have very low energy (mainly protons, with energies of a few keV) and are easily shielded by Earth's magnetosphere. In the polar regions, where the magnetic shielding is weak, the particles range out in the thermosphere at an altitude of about 100 km. This is far from the troposphere—the layer of the atmosphere most responsible for Earth's climate—which lies below about 10–15 km altitude.

Since variations of total solar irradiance appear to be too low to account for observed climate variations, attention has focused on changes of the UV component of the solar spectrum [Haigh, 1996, Larkin *et al.*, 2000] which, although it carries only a small fraction of the total energy (about 0.1%), shows a much larger variation of several per cent over the solar cycle. The UV spectrum is absorbed at altitudes above 30 km by oxygen (<240 nm wavelength) and ozone (200–300 nm), and causes measurable heating of the thin atmosphere in the upper stratosphere. A positive feedback mechanism exists since the increased UV creates more ozone and therefore more UV absorption. However, the measured change of ozone concentration from solar minimum to maximum is small (about 1–2%). Modelling reproduces these variations, and some studies (e.g. [Shindell, 1999]) suggest that the resultant changes in stratospheric heating and circulation could dynamically and radiatively couple to the troposphere, which could in turn influence cloudiness.

In contrast with solar UV radiation, GCRs directly penetrate the lower troposphere where the cloud variation is observed, and they have an appreciable intensity variation over the solar cycle (§3.2). At low altitudes over land (<1 km), natural radioactivity contributes about 20% of atmospheric ionisation. Over oceans, the contribution of radioisotopes is negligible and so, averaged over the entire troposphere, GCRs are by far the dominant source of ionisation (more than 99%).

The data presented in §4 show that GCR variations are clearly connected with past climate change. However the interpretation is often ambiguous; this may indicate either a direct effect of GCRs on the climate or else the GCRs may merely be acting as a proxy for solar irradiance/UV changes. In principle, this ambiguity can be resolved since,

on longer time scales, the GCR intensity is also affected by the geomagnetic field and by the galactic environment (§3.2), whereas the solar irradiance/UV is not. Indeed, there is suggestive evidence linking the climate both with the geomagnetic field and with the galactic environment (§4). For the remainder of this paper, we will focus on a possible direct influence of cosmic rays on the climate.

3.2 Cosmic Ray Modulation

Cosmic rays are accelerated by supernovae and other energetic sources in our galaxy. On entering the heliosphere, charged cosmic rays are deflected by the magnetic fields of the solar wind. The transport problem of the GCRs through the heliosphere was first solved by Parker (1965). It involves several processes of which the dominant is scattering off the magnetic irregularities, which produces a random walk or diffusion effect. It has been shown theoretically that the heliospheric shielding can be approximated by an equivalent heliocentric retarding (i.e. decelerating) electric potential [Gleeson and Axford, 1967]. This retarding potential varies between about 1000 MV during periods of very high solar activity and zero during grand minima such as the Maunder Minimum. The solar wind therefore partly shields the Earth from the lower energy GCRs and affects the flux at energies below about 10 GeV. The effective retarding potential over the present eleven-year solar cycle averages about 550 MV, ranging from about 450 MV at the minimum to 850 MV at maximum. This leads to a distinct solar modulation of the GCR intensity (Fig. 12.3).

The geomagnetic field also partially shields the Earth from GCRs. The dipole field imposes a minimum vertical momentum of about 13 GeV/c at the equator, 3 GeV/c at mid latitudes, and falling essentially to zero at the geomagnetic poles. In consequence, the GCR intensity is about a factor 3.6 higher at the poles than at the equator, and there is a more marked solar cycle variation at higher latitudes. Over the solar cycle, the variation of GCR intensity at the top of the atmosphere is about 15%, globally averaged, and ranges from ∼5% near the geomagnetic equator to ∼50% at the poles (Fig. 12.3). At lower altitudes both the GCR intensity and its fractional solar modulation decrease. These are consequences of the absorption of low energy GCRs and their secondary particles by the atmospheric material, which totals about 11 nuclear interaction lengths. Balloon measurements (Fig. 12.4) show solar cycle variations of about 10% at low altitudes around 3 km (for a 2.4 GeV/c rigidity cutoff).

The sources of GCR modulation are summarised in Table 12.1. On the longest timescales, the GCR intensity is modulated by passage through

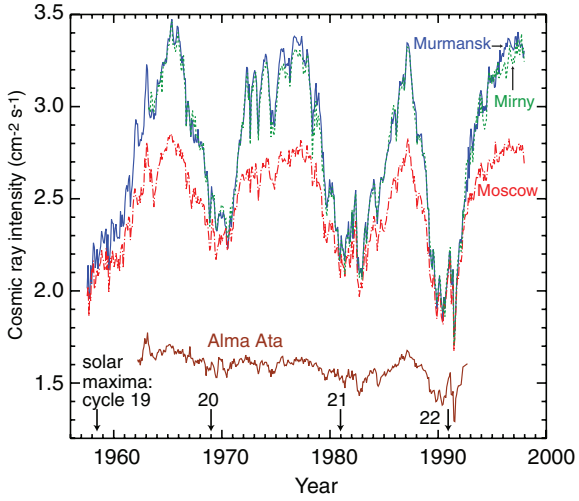

Figure 12.3. Balloon measurements of the cosmic ray intensity at shower maximum (15–20 km altitude) for the period 1957–1998, measured by the Lebedev Physical Institute. The curves correspond to four different locations for the balloon flights: Mirny-Antarctica (0.03 GeV/c rigidity cutoff), Murmansk (0.6 GeV/c), Moscow (2.4 GeV/c) and Alma-Ata (6.7 GeV/c). Due to atmospheric absorption, the data of Murmansk and Mirny practically coincide with each other. The approximate times of the sunspot maxima for the last 4 solar cycles are indicated.

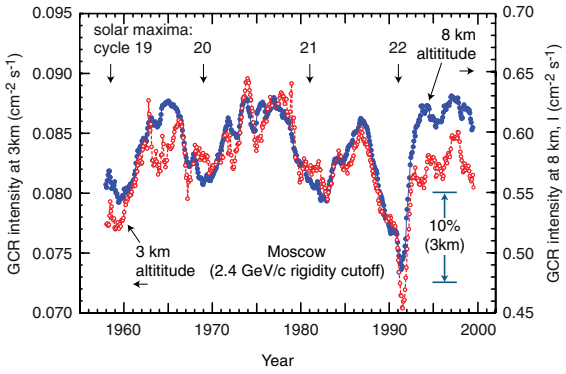

Figure 12.4. Balloon measurements of the GCR intensity at 3 km and 8 km altitudes from 1957 to 2000 (2.4 GeV/c rigidity cutoff), measured by the Lebedev Physical Institute. The approximate dates of the sunspot maxima for the last 4 solar cycles are indicated.

Table 12.1. Sources of GCR Modulation and their Typical Characteristics.

Source	*Variability timescale*	*GCR change*
Solar wind	10 yr – 1 kyr	±10–30%
Geomagnetic field	100 yr – 100 Myr	±20–100%
Galactic variations	>10 Myr	±50–100%

the spiral arms of the Milky Way [Shaviv, 2002]. The local GCR intensity is higher within the spiral arms owing to the relative proximity of the supernovae generators and the subsequent diffusive trapping of the energetic charged particles by the interstellar magnetic fields. Superimposed on this diffuse GCR rate are possible isolated events caused by nearby supernovae. For example, evidence has recently been obtained for an enhancement in the fraction of the ^{60}Fe radio-isotope ($\tau_{1/2}$ = 1.5 Myr) in a deep-sea ferromagnetic crust [Knie *et al.*, 2004]. This suggests a nearby supernova, at a distance of several 10's pc, which increased the GCR intensity by ∼15% for a few 100 kyr around 2.8 Myr ago.

3.3 Cosmic Ray Archives

On reaching Earth, cosmic rays interact with nuclei in the atmosphere, creating showers of secondary particles, and dissipating energy by ionisation. Among the products are light radio-isotopes, of which the two most abundant are ^{14}C ($\tau_{1/2}$ = 5730 yr; global mean production rate ∼2.0 atoms cm^{-2}s^{-1}) and ^{10}Be (1.5 Myr; ∼1.8×10^{-2} atoms cm^{-2}s^{-1}). These settle on the surface of Earth either via the carbon cycle ($^{14}CO_2$) or in rain and snow (^{10}Be). Since this is their only terrestrial source, the resultant archives of light radio-isotopes found in tree rings, ice cores and marine sediments provide direct records of the past GCR flux. For the long-lifetime ^{10}Be, these records at present go back about 1 Myr, and are likely to be extended in future.

Once produced, ^{14}C is rapidly oxidised to $^{14}CO_2$. The turnover time of CO_2 in the atmosphere is quite short—about 4 years—mostly by absorption in the oceans and assimilation in living plants. However, because of recirculation between the oceans and the atmosphere, changes in the ^{14}C fraction on timescales less than a few decades are smoothed out. Plant material originally contains the prevailing atmospheric fraction of ^{14}C and, subsequently, since the material is not recycled into the atmosphere, the fraction decreases with the characteristic half life of ^{14}C. By analysing the ^{14}C content in the rings of long-lived trees such as the California bristlecone pine, and also ancient tree samples, a detailed record of GCR intensity over the last 40 kyr has been assembled.

In the case of ^{10}Be [Beer, 2000], after production it rapidly attaches to aerosols and follows the motion of the surrounding air masses. Since the production of ^{10}Be follows the intensity profile of the cosmic ray hadronic showers, about 2/3 is produced in the stratosphere and 1/3 in the troposphere, globally averaged. Due to the tropopause barrier, aerosols in the stratosphere take about 1–2 years to settle on the Earth's surface, whereas the mean residence time in the troposphere is only about a week. If the sedimentation occurs in the form of snow in a permanently frozen and stable region such as Greenland or Antarctica then the subsequent compacted ice preserves a temporal record in layers according to their depth. If, on the other hand, sedimentation occurs into rivers and oceans, then eventually (after about 1000 yr mean time) the ^{10}Be settles in ocean sediments. Cores retrieved from polar ice or the ocean floor thereby constitute an archive of past GCR intensity. Ice cores have the advantage of higher time resolution, whereas ocean sediments provide longer time records and a globally-averaged measurement.

3.4 Climate Archives

Many ingenious proxies have been developed to reconstruct the climate prior to the instrumental record of the last 150 years. Cultural records over the last millennium are an important source since humans are sensitive to climate change, especially when prolonged drought, cold or flooding is involved. These documents include the dates when the first cherry blossoms appeared each spring in China, the records of grape harvests in Europe, and the waxing and waning of Alpine glaciers. Other records (with their approximate time span before present) are tree rings (10 kyr), mosses (10 kyr), coral terraces (500 kyr), ice cores (700 kyr), speleothems (1 Myr), loess deposits (wind-blown silt; 1 Myr), pollens (1 Myr), ocean sediments (>500 Myr) and geomorphology (4 Byr).

Ice cores are an especially valuable record of past climate since they have high resolution and excellent preservation of a wide range of climatically-sensitive material. Trapped air bubbles preserve the atmospheric composition at earlier times, measuring gases such as carbon dioxide (ocean ventilation, volcanic and biomass activity), methane (wetland extent), deuterium (temperature), nitrous oxide (bacterial activity and stratospheric air exchange) and methanesulphonic acid (phytoplankton activity); layer thicknesses measure precipitation rate; dust content measures wind, aridity, land biota and volcanic activity; the radio-isotope ^{10}Be measures solar/GCR activity; non-sea-salt sulphate measures sulphuric acid content of the atmosphere (phytoplankton and volcanic activity); nitrates measure ionising radiation (UV and cosmic

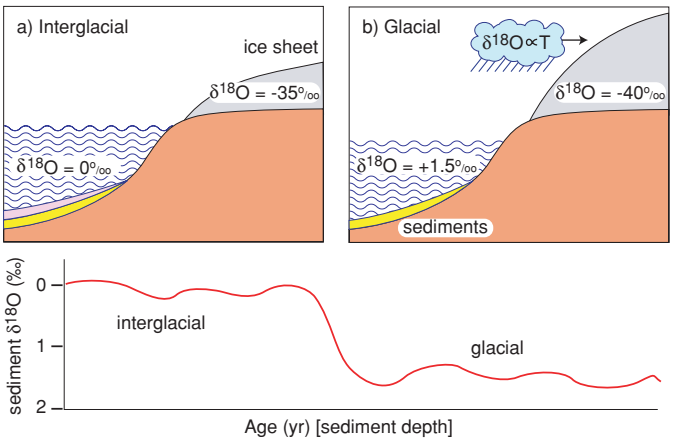

Figure 12.5. Principle of the global ice volume proxy obtained from the ^{18}O fraction in ocean sediments (lower panel) during a) interglacial and b) glacial conditions. The physical basis for proxy temperature measurements from the stable ^{18}O isotope is that the vapour pressure of $H_2{}^{18}O$ is lower than that of $H_2{}^{16}O$. Evaporated water is therefore ^{18}O-depleted and the subsequent rainfall from a cloud progressively reduces the ^{18}O fraction of the remaining water vapour. Ice formed from snow is therefore isotopically light (depleted in ^{18}O)—and even lighter during glacial climates since the lower temperatures further deplete the clouds of ^{18}O. A large global ice volume therefore leaves the oceans relatively enriched in ^{18}O. Since the prevailing isotopic fraction of the water is transferred to organisms living in the oceans, the ^{18}O fraction found in ocean sediments provides a proxy for global ice volume.

ray bursts); and, of particular importance, the stable ^{18}O isotope measures past temperatures, rainfall and global ice volume (Fig. 12.5).

4. Solar/GCR-climate Variability

The GCR and climate archives provide extensive evidence for significant correlations between cosmic ray flux and climate, on both short and long time scales. The pattern is summarised in Table 12.2. We will present a brief review of solar/GCR-climate observations in this section, progressively looking further back in time.

Table 12.2. Observed Correlation of Cosmic Rays and Climate.

Cosmic ray flux	*Climate*
high	cool
low	warm

4.1 Twentieth century

Global cloud cover. Based on satellite data from the ISCCP [Rossow, 1996], Svensmark *et al.* have reported a correlation between GCR intensity and the fraction of Earth covered by low clouds (Fig.12.6b) [Svensmark and Friis-Christensen, 1997, Marsh and Svensmark, 2003]. These correlations have been subjected to intense scrutiny and criticism (e.g. [Kernthaler *et al.*, 1999, and others]). The measurements are difficult, involving the inter-calibration of instruments on board several geostationary satellites and polar-orbiting satellites, over a period of 20 years. The low-cloud data appear to show a poor correlation with GCR intensity after 1994 (or perhaps a GCR modulation superimposed on a linearly-decreasing trend). However, questions have been raised about an apparent break in the cloud measurements at the end of 1994 (Figs. 12.6a and b) which coincides with a period of a few months during which no polar-orbiting satellite was available for inter-calibration [Marsh and Svensmark, 2003].

Although not conclusive, the low cloud data nevertheless suggest a significant solar imprint. The low cloud modulation represents around 1 Wm^{-2} variation in net radiative forcing at Earth's surface over the solar cycle, which is about a factor 5 larger than the variation of solar irradiance (§2.2.0). Furthermore, the two effects are in phase; increased sunspot activity corresponds to increased irradiance, decreased GCR

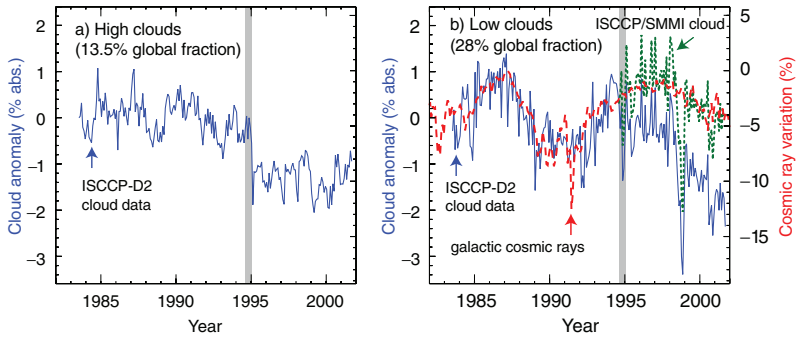

Figure 12.6. Satellite measurements of global cloud anomalies over the last 20 years: a) high clouds (above about 6.5 km), and b) low clouds (below about 3.2 km) [Marsh and Svensmark, 2003]. The vertical grey bar around the end of 1994 corresponds to a period without any polar-orbiting satellite available to inter-calibrate the geostationary satellites used for the ISCCP cloud measurements. In panel b) the dashed red curve shows the variation of GCR intensity, and the dotted green curve shows the ISCCP data after correcting by its difference with SMMI cloud data after 1994.

intensity and decreased low cloud amount. Since low clouds have a net cooling effect, this implies increased radiative forcing and a warmer climate. Finally, Usoskin *et al.* (2004) report that the solar/GCR-cloud correlation shows some evidence for an increased amplitude at higher latitudes. Since the GCR intensity and modulation is more pronounced at higher latitudes, whereas solar/UV intensity variations are the same at all latitudes, this observation favours a GCR mechanism rather than a solar/UV effect.

Sea surface temperatures. An important component of the temperature reconstruction during the current warming is sea-surface temperatures (SSTs), which have been measured on a routine basis by ocean-going ships since the mid 19^{th} century. The SST record is a particularly valuable measure of global climate since it represents over 70% of Earth's surface and is much more spatially and temporally homogeneous than the land surface. It is also free of the uncertainties of temperature increases arising from population growth in 'urban heat islands'. The mean SSTs over the period 1860–1985 for the Atlantic, Pacific and Indian Oceans are shown in Fig. 12.7, together with the global mean SST [Reid, 1987]. All oceans show a temperature rise that levels off in the

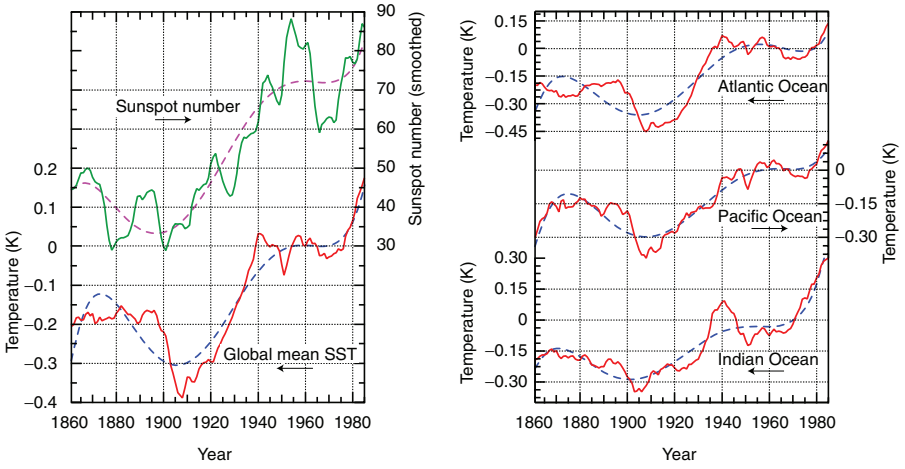

Figure 12.7. Annual mean sea-surface temperatures (SST), 1860–1985, for the Atlantic, Pacific and Indian Oceans (right-hand panel) and the global mean (lower curve in the left-hand panel) [Reid, 1987]. The temperatures are shown relative to their 1951–1980 averages. Also shown is the 11-year running mean of the annual sunspot numbers (upper curve in the left-hand panel). The smooth dashed curves are 7^{th} order polynomial fits to the data.

same period around 1945–1980, as well as a cooling around the beginning of the last century. Both of these features are characteristic of solar activity and GCR intensity, as can be seen in the smoothed sunspot number (Fig. 12.7).

A world-wide simultaneous variation of SST puts severe constraints on a possible forcing mechanism. Since the same characteristic features are seen in all oceans, they are unlikely to be caused by changes such as El Niño events, shifts in wind patterns or changes in the thermohaline circulation, which would lead to differences between the oceans. The mechanism could in principle be increases of anthropogenic greenhouse gases, but the variation in the first half of the 20^{th} century occurred before these were significant. There were insufficient volcanic events to account for the mid-century cooling. In conclusion, these data provide quite strong evidence that solar variability was the primary cause of the warming during at least the first half of the last century. Indeed, this is now accepted by general circulation models. However, the apparent good agreement has recently been thrown into doubt since the climate models use reconstructions of irradiance variations (e.g. [Lean *et al.*, 1995]) that may be over-estimated by a factor of five (§2.2.0).

4.2 Last millennium

Numerous palaeoclimatic reconstructions have shown evidence for a Medieval Warm period between about 1000 and 1270, followed by a prolonged cold period known as the Little Ice Age between about 1450 and 1850. Temperatures during the Medieval Warm period were elevated above normal, allowing the Vikings to colonise Greenland and wine-making to flourish in England. It was followed by a period of about 4 centuries during which—save for a few short interruptions—the glaciers advanced and a cooler, harsher climate predominated.

A recent multi-proxy reconstruction of Northern Hemisphere temperatures estimates that the Little Ice Age was about 0.7 K below the 1961–1990 average, and that climate during the Medieval Warm period was comparable to the present (Fig. 12.8a) [Moberg *et al.*, 2005]. This reconstruction contrasts with a widely-quoted earlier reconstruction [Mann *et al.*, 1998, Mann *et al.*, 1999], known as the *hockey-stick* curve, which shows a rather flat temperature variation prior to 1900 (Fig. 12.8a). However the methodology of the principal-component analysis used to derive the hockey-stick curve has recently been questioned and, when properly analysed, the data show larger long-term temperature variations, characteristic of the Little Ice Age and Medieval Warm period [McIntyre and McKitrick, 2005].

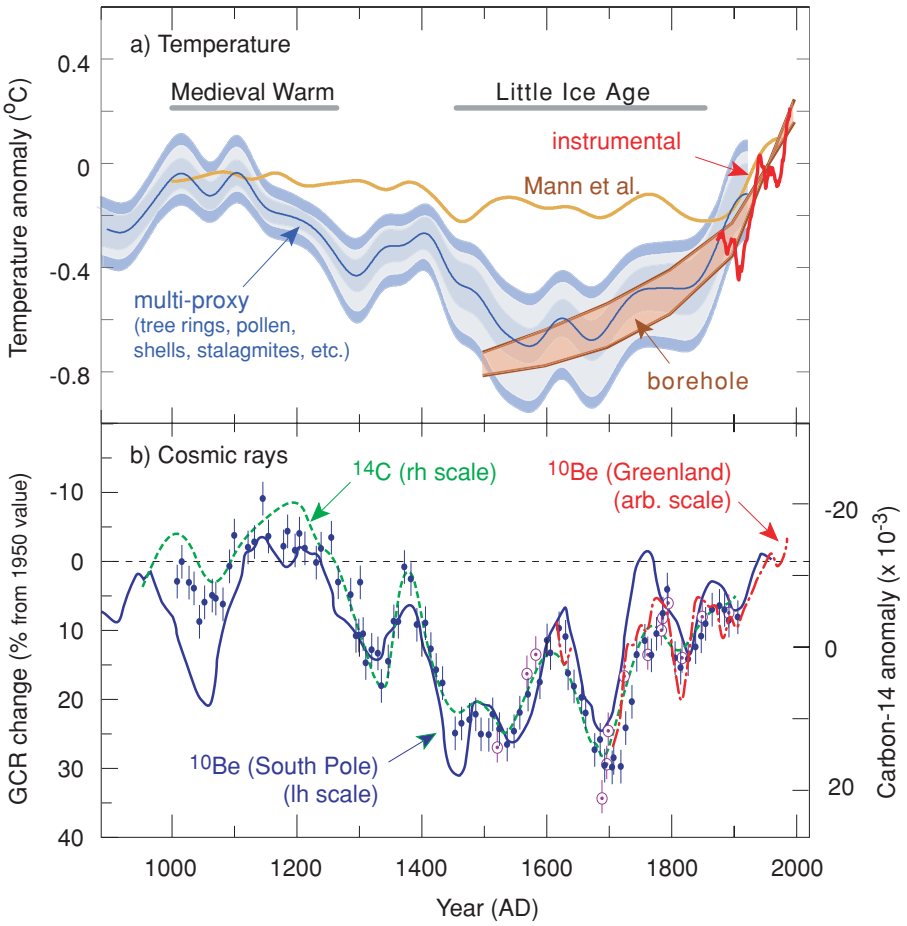

Figure 12.8. Comparison of variations during the last millennium of a) temperature (with respect to the 1961–1990 average) and b) galactic cosmic rays (note the inverted scale; high cosmic ray fluxes are associated with cold temperatures). The temperature curves comprise a recent multi-proxy reconstruction of northern hemisphere temperatures (the full band shows the 95% confidence interval; [Moberg *et al.*, 2005]), the so-called 'hockey-stick' curve [Mann *et al.*, 1998, Mann *et al.*, 1999], borehole temperature measurements [Pollack and Smerdon, 2004], and smoothed instrumental measurements since 1860. The cosmic ray reconstructions are based on several ^{14}C measurements: tree rings (shown by the data points and the dashed green curve) [Klein *et al.*, 1980], and ^{10}Be concentrations in ice cores from the South Pole (solid blue curve) [Raisbeck *et al.*, 1990] and Greenland (dot-dashed red curve) [Usoskin *et al.*, 2002].

The variation of GCR intensity over the last millennium is shown in Fig. 12.8b), as reconstructed from ^{14}C in tree rings, and ^{10}Be in ice cores from the South Pole and Greenland. Close similarities are evident between the temperature and GCR records. Most of the GCR variation over this period is due to solar magnetic variability (see, for example, Fig. 12.1), so these data cannot distinguish between a direct effect of GCRs on climate, or a GCR proxy for solar irradiance/UV.

4.3 Holocene

Indian Ocean monsoon. Neff *et al.* (2001) have measured the δ^{18}O composition in the layers of a stalagmite from a cave in Oman, which are U-Th dated to cover the period from 9,600 to 6,200 yr BP. The δ^{18}O is measured in calcium carbonate, which was deposited in isotopic equilibrium with the water that flowed at the time of formation of the stalagmite. The data are shown in Fig. 12.9 together with Δ^{14}C measured in tree rings such as the California bristlecone pine. The two

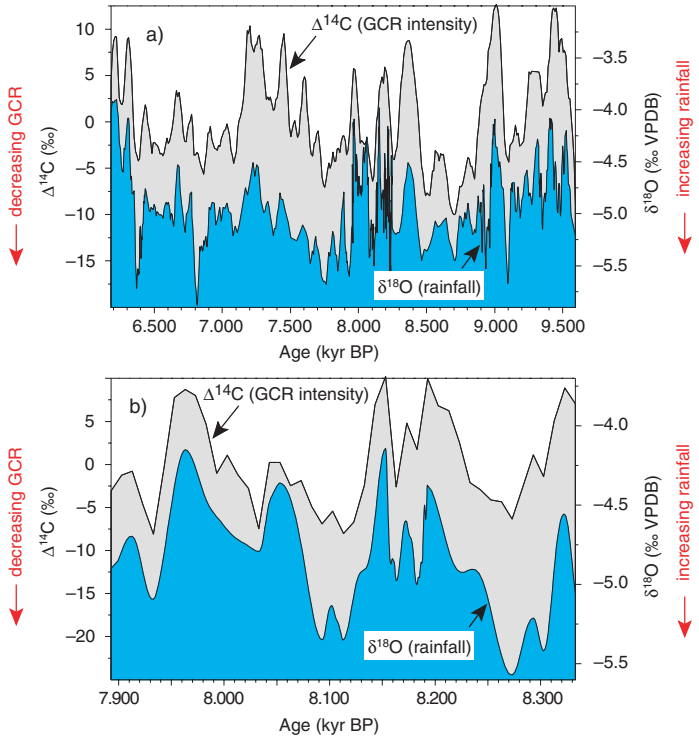

Figure 12.9. A comparison of variations of δ^{18}O in a U-Th-dated stalagmite from a cave in Oman with variations of Δ^{14}C from tree rings elsewhere in the world, for a) the 3.4 kyr period from 9,600 to 6,200 yr BP and b) the 430 yr period from 8,330 to 7,900 yr BP [Neff *et al.*, 2001].

timescales have been tuned to match bumps within the known experimental errors (smooth shifts have been applied to the U-Th dates up to a maximum of 190 yr). During a 430-yr period centred around 8.1 kyr BP, the stalagmite grew at a rate of 0.55 mm/yr—an order of magnitude faster than at other times—which allowed a high resolution δ^{18}O measurement to be made (Fig. 12.9b).

Oman today has an arid climate and lies beyond the most northerly excursion of the inter tropical convergence zone (ITCZ), which determines the region of heavy rainfall of the Indian Ocean monsoon system. However there is evidence that the northern migration of the ITCZ reached higher latitudes at earlier times and, in consequence, that Oman had a wetter climate. In this region, the temperature shifts during the Holocene are estimated to account for only 0.25 per mil variation in δ^{18}O [Neff *et al.*, 2001]. However the δ^{18}O values of monsoonal rainfall associated with the ITCZ show an inverse correlation with amount of rainfall (increased rainfall results in a decreased ^{18}O fraction; see Fig. 12.5). For these data, the δ^{18}O variations are therefore ascribed to changes of rainfall. Higher rainfall is associated with reduced GCR intensity (Fig. 12.9).

The striking similarity between the δ^{18}O and Δ^{14}C data indicates that that solar/GCR activity tightly controlled the monsoon rainfall of the Indian Ocean region during this 3,000-year period.

Ice-rafted debris in the North Atlantic. Bond *et al.* have analysed sediments of ice rafted debris (IRD) in the North Atlantic [Bond *et al.*, 1997a, Bond *et al.*, 1997b, Bond *et al.*, 2001]. The latter are found in deep sea cores as layers of tiny stones and micro-fossils that were frozen into the bases of advancing glaciers and then rafted out to sea by glaciers. These reveal abrupt episodes when cool, ice-bearing waters from the North Atlantic advanced as far south as the latitude of southern Britain, coincident with changes in the atmospheric circulation recorded in Greenland. A quasi-cyclic occurrence of IRD events with a periodicity of 1470 ± 530 yr has been found, during which temperatures dropped and glacial calving suddenly increased (Fig. 12.10).

Until recently the trigger for this millennial-scale climate cycle was unknown. Orbital periodicities around the Sun are too long to cause millennial-scale climate cycles (see Fig. 12.14). There are several reasons to rule out ice sheet oscillations as the forcing mechanism. First, the rafting icebergs are launched simultaneously from more than one glacier, and so the driving mechanism cannot be ascribed to a single ice sheet. It requires a common climate forcing mechanism that induces the release of ice over a large region. Second, the events continue with the same periodicity through at least three major climate transitions: the Younger Dryas-Holocene transition, the glacial-interglacial transition, and the

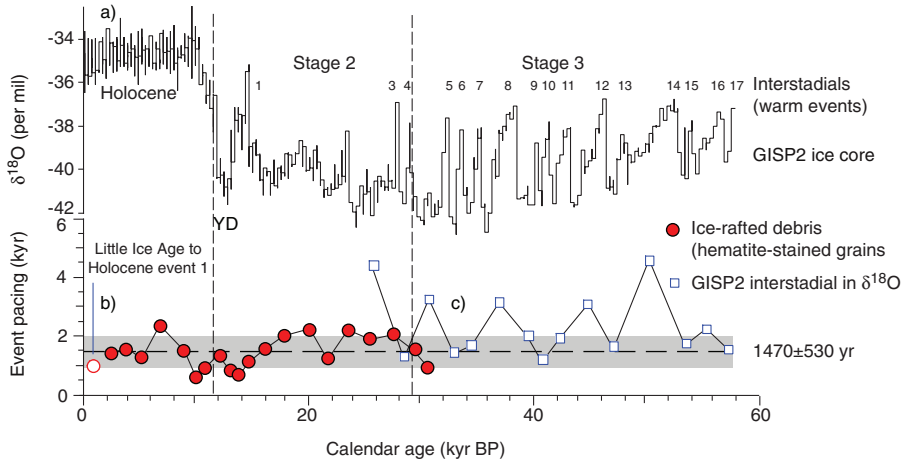

Figure 12.10. Periodicity of ice rafted debris (IRD) events in the North Atlantic [Bond *et al.*, 1997b]. The curves show a) the GISP2 ice core δ^{18}O record of Greenland temperatures over the last 60 kyr (Holocene, late glacial/Stage 2 and mid glacial/Stage 3 periods), b) the periodicity of IRD events from 32 kyr BP to the present, measured from haematite-stained grains (other tracers give similar results), and c) the periodicity of Dansgaard-Oeschger warm events in the GISP2 δ^{18}O data from 58 kyr to 26 kyr BP.

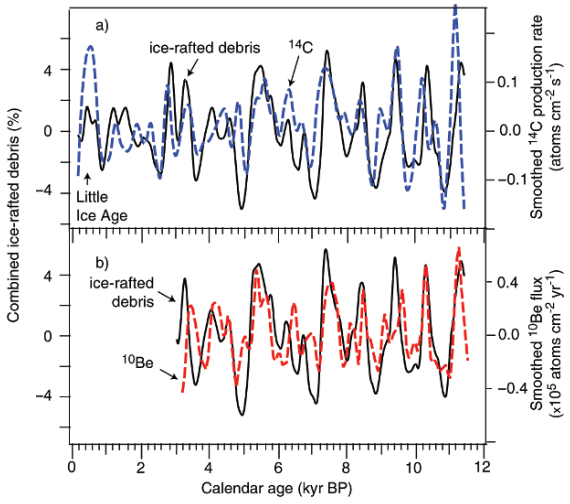

Figure 12.11. Correlation of solar/GCR variability (dashed curves) with ice-rafted debris (solid curves) in the North Atlantic during the Holocene [Bond *et al.*, 2001]: a) the ^{14}C cosmic ray record (correlation coefficient 0.44) and b) the ^{10}Be cosmic ray record (0.56), together with the combined ice-rafted-debris tracers. The Little Ice Age is indicated in the upper panel.

boundary within the glacial age between the marine isotope stages 2 and 3. Even though the ice conditions during these transitions were changing dramatically, the IRD events continued with the same periodicity.

Third, and especially surprising, is the evidence that the IRD cold events have continued through the Holocene (Fig. 12.10), with the same periodicity (but with a lower amount of IRD material). The events were abrupt during both the glacial and Holocene periods, generally switching on and off within one or two centuries. The estimated decreases in North Atlantic Ocean temperatures during the Holocene IRD events are 2 K, or about 15–20% of the full Holocene-to-glacial temperature difference.

A recent study has shown that solar/GCR variability is highly correlated with the ice rafted debris events during the Holocene phase (Fig. 12.11) [Bond *et al.*, 2001]. This correlation between high GCR flux and cold North Atlantic temperatures embraces the Little Ice Age, which is seen not as an isolated event but rather as the most recent of around ten such events during the Holocene. A high GCR flux is associated with a cold climate, and a low flux with a warm climate. On these 100 yr timescales, variations of the cosmic ray flux are thought to reflect changing solar activity. However, recent high-resolution palaeomagnetic studies suggest that short-term geomagnetic variability may in fact control a significant fraction of the GCR modulation within the Holocene, even on 100 yr timescales [St-Onge *et al.*, 2003]. This suggests that GCRs directly influence the climate, rather than merely serve as a proxy for solar variability.

Figure 12.11 provides convincing evidence that solar/GCR forcing is responsible for at least the Holocene phase of this 1500 yr climate cycle. Moreover, the similarity of the pacing of these events with the warm Dansgaard-Oeschger events during the ice age suggests that they too may be initiated by solar/GCR forcing. In this case, changes of North Atlantic Deep Water (NADW) production are a positive feedback in response to the solar/GCR forcing, rather than being the primary driver of climate change. Simulations [Ganopolski and Rahmstorf, 2001] show that a small decrease of freshwater into the North Atlantic is sufficient to increase salinity of the North Atlantic and trigger the 'warm' heat conveyor mode with NADW formation further north, in the Nordic Seas. This would suggest that solar/GCR forcing may have initially modified the hydrological cycle in the North Atlantic region, which then triggered the warm NADW mode.

Biogenic activity in the North Pacific region. Recent evidence shows that that these millennial scale shifts in Holocene climate were also present in the sub-polar North Pacific [Hu *et al.*, 2003]. Variations

of biogenic silica were measured in the sediment from Arolik Lake in a tundra region of south-western Alaska. Biogenic silica reflects the sedimentary abundance of diatoms—single-celled algae which dominate lake primary productivity. High-resolution analyses reveal cyclic variations in climate and ecosystems during the Holocene with periodicities similar to those of the North Alantic drift ice and the cosmogenic nuclides ^{14}C and ^{10}Be (Fig. 12.12). High GCR flux is associated with low biogenic activity. Taken together, these results imply that solar/GCR forcing of Holocene climate occurred over a large fraction of the high-latitude northern region.

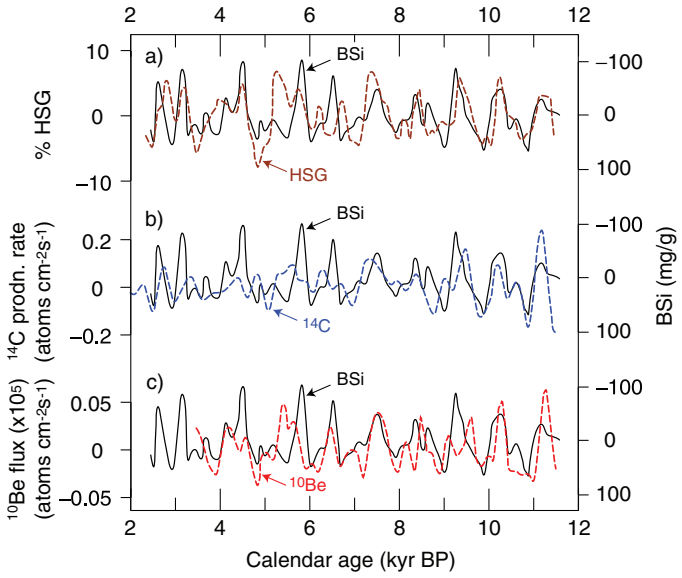

Figure 12.12. Correlation of solar/GCR variability with the biogenic silica (BSi) record from Arolik Lake in sub-polar Alaska [Hu *et al.*, 2003]: a) percentage of haemetite-stained grains (HSG) found in North Atlantic ice-rafted debris (dashed brown curve) c), b) ^{14}C production rate (dashed blue curve) and c) ^{10}Be flux (dashed red curve). BSi measures the level of biogenic activity in the lake, and is shown as the solid black line in all three plots (note the inverted scale; high cosmic rays are associated with low biogenic activity). All data are detrended and smoothed.

4.4 Ice ages

The most important clue for identifying the cause of the glacial cycles is the spectral purity of their periodicity [Muller and McDonald, 2000]. For the past million years, the glacial pattern is dominated by a precise 100 kyr cycle, and for the million years before that, by an equally precise 41 kyr cycle (Fig. 12.13). These match the major frequencies of

Earth's orbital cycles (Fig. 12.14), and so it is generally accepted that the primary driver for the ice ages was astronomical. A linkage between orbit and climate is provided by the Milankovitch model, which states that melting of the northern ice sheets is driven by peaks in Northern Hemisphere summer insolation (solar heating). This has become established as the standard model of the ice ages since it naturally includes spectral components at the orbital modulation frequencies.

However, high precision palaeoclimatic data have revealed serious discrepancies with the Milankovitch model that fundamentally challenge its validity and re-open the question of what causes the glacial cycles [Muller and McDonald, 2000]. It has been proposed that cosmic rays are

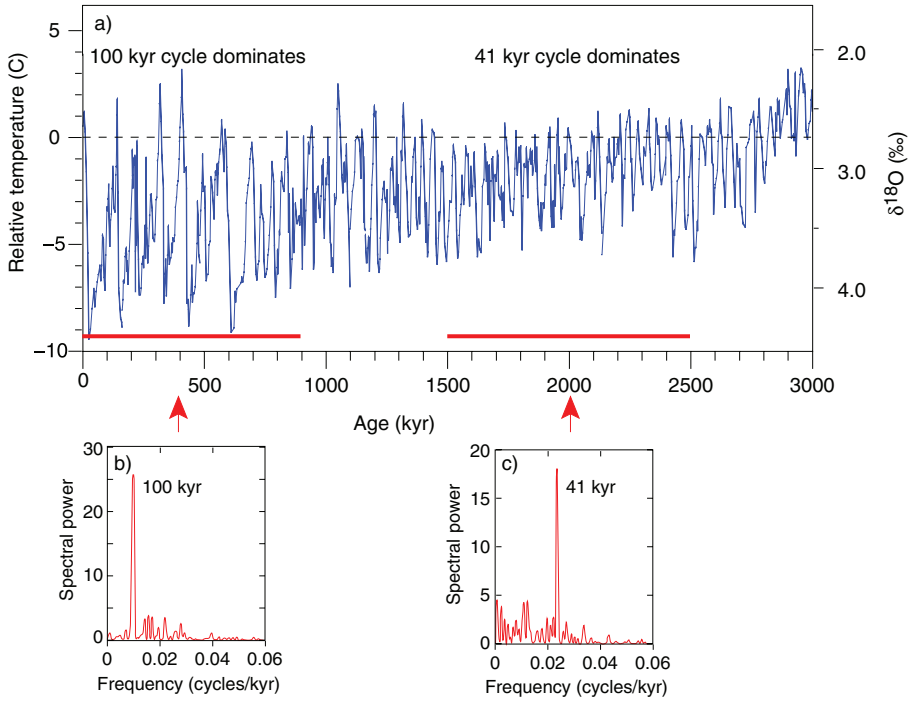

Figure 12.13. a) Climate for the last 3 Myr, as derived from the benthic δ^{18}O record from DSDP site 607 in the North Atlantic. For the past 1 Myr, climate has followed a precise 100-kyr cycle, and prior to that, an equally-precise 41 kyr cycle, as seen in the two periodograms: b) spectral power for ODP site 659, from 0 to 900 kyr and c) spectral power for DSDP site 607, from 1.5 to 2.5 Myr [Muller and McDonald, 1997]. The time scale for both periodograms assumes a constant sedimentation rate, i.e. the data are untuned. The narrow spectral widths imply that the glacial cycles are driven by an astronomical force, regardless of the detailed mechanism; oscillations purely internal to Earth's climate system could not maintain such precise phase coherency.

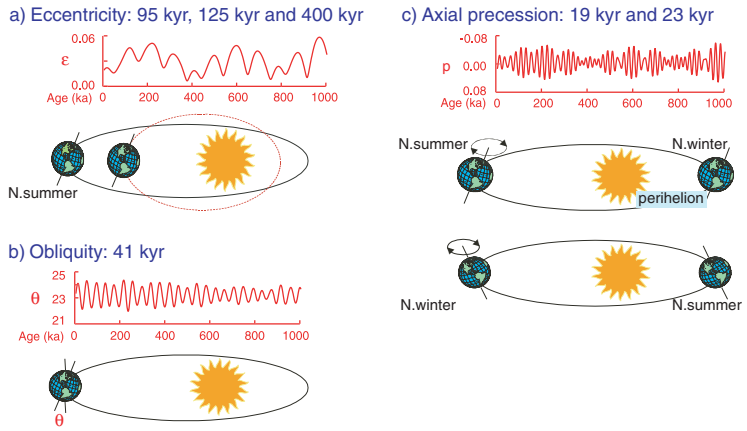

Figure 12.14. Earth's orbital cycles (caused by the gravitational pulls of the planets and by gravitational torques exerted on Earth's equatorial bulge): a) eccentricity (95, 125 and 400 kyr periodicity): the departure of Earth's orbit from a perfect circle, b) obliquity (41 kyr): the angle of tilt of Earth's axis towards the Sun, which affects the seasonal insolation contrast, and c) precession (19 and 23 kyr): the 'wobble' of Earth's axis with respect to the stars, which causes the perihelion (position of closest approach to the Sun) to cycle through the seasons.

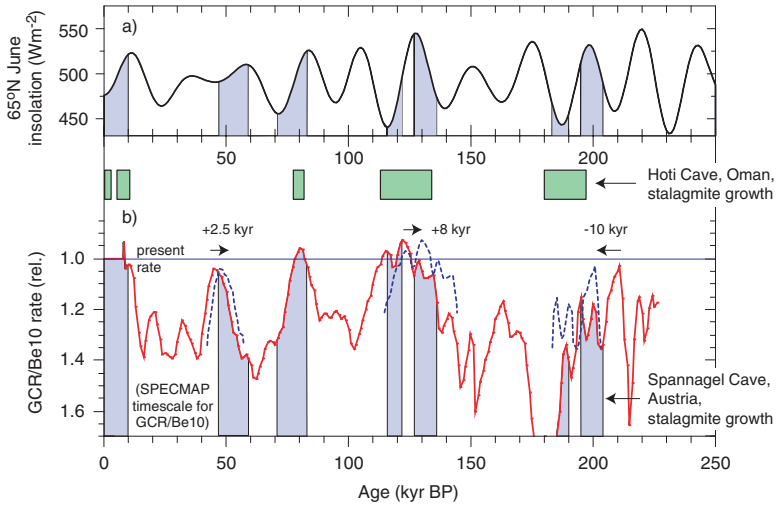

Figure 12.15. Comparison of the growth periods of stalagmites in Austria and Oman with a) 65°N June insolation and b) the relative GCR flux (^{10}Be ocean sediments; note inverted scale) [Christl *et al.*, 2004, Kirkby *et al.*, 2004]. The growth periods are indicated by shaded bands (Spannagel cave) or boxes (Hoti cave). Growth periods at Spannagel cave require warm temperatures, close to the present climate; growth periods at Hoti cave require a moist climate. Periods without stalagmite growth are unshaded. The dashed curves in b) indicate the estimated corrections of systematic errors in the SPECMAP timescale, on which the GCR record is based. The growth periods are associated with intervals of low GCR flux, close to present values.

a primary trigger of glacial-interglacial conditions [Kirkby *et al.*, 2004]. This proposal is based on a wide range of evidence, some of which is discussed in this paper, including the records of speleothem growth in caves in Austria and Oman [Christl *et al.*, 2004], and the record of cosmic ray flux over the past 220 kyr obtained from the ^{10}Be composition of deep-ocean sediments [Christl *et al.*, 2003] (Fig. 12.15).

The measurements of ^{10}Be production show that the GCR flux over the last 220 kyr was generally around 20–40% higher than today, due to a reduced geomagnetic field. However there were several relatively short periods when the GCR flux returned to present levels. During these periods, stalagmite growth was observed in the Austrian and Oman caves. The growth of stalagmites at each of these locations is especially sensitive to climate since it requires temperatures at least as warm as today's (within 1.5±1°C). In contrast, the stalagmite growth periods show no clear pattern of association with 65°N June insolation, contrary to the expectations of the standard Milankovitch model (Fig. 12.15a).

A further problem for the Milankovitch model concerns the timing of Termination II—the penultimate deglaciation. The growth period of stalagmite SPA 52 from Spannagel Cave began at 135±1.2 kyr [Spötl *et al.*, 2002] (Fig. 12.15b). So, by that time, temperatures in central Europe were within 1°C or so of the present day. This corroborates Henderson and Slowey's conclusion, based on sediment cores off the Bahamas, that warming was well underway at 135±2.5 kyr [Henderson and Slowey, 2000]. Furthermore, dating of a Barbados coral terrace shows that the sea level had risen to within 20% of its peak value by 135.8±0.8 kyr [Gallup *et al.*, 2002]. These results confirm the 'early' timing of Termination II, originally discovered at Devil's Hole Cave, Nevada, by Winograd *et al.* (1992). In summary, the warming at the end of the penultimate ice age was underway at the *minimum* of 65°N June insolation, and essentially complete about 8 kyr prior to the insolation maximum (Fig. 12.15a). The Milankovitch model therefore suffers a causality problem at Termination II: the deglaciation precedes its supposed cause. Furthermore, based on an analysis of deep ocean cores, Visser *et al.* (2003) report that warming of the tropical Pacific Ocean at Termination II preceded the northern ice sheet melting by 2–3 kyr. So the northern ice sheets were not the primary driver of the penultimate deglaciation—contrary to the expectations of the Milankovitch model—but rather a response to some other initial forcing.

The ^{10}Be data, on the other hand, show that the GCR flux began to decrease around 150 kyr, and had reached present levels by about 135 kyr (Fig. 12.15b). This is compatible with Termination II being driven in part by a reduction of cosmic ray flux—albeit within large experimental

errors. A similar reduction of GCR flux also occurred around 20 kyr BP due to a rise in the geomagnetic field strength towards present values. This was coincident with the first signs of warming at the end of the last glaciation, as recorded in the Antarctic ice at about 18 kyr BP.

At present the GCR archive data do not have the precision to compare to the spectral purity observed in the climate record (Fig. 12.13). Moreover, a mechanism would be needed to explain how the orbital cycles could be imprinted on the GCR intensity. One possibility would be an orbital influence on the geomagnetic field. Indeed, some measurements suggest that long-term records of variations of Earth's magnetic field—in both strength and magnetic inclination—show the presence of orbital frequencies [Channell *et al.*, 1998, Yamazaki and Oda, 2002]. The effects persist when the archives are corrected for climatic influences. Although it is speculative that orbital variations could modulate the Earth's dipole field, such a linkage is plausible.

If cosmic rays are indeed affecting climate on glacial time scales, then there are definite predictions that can be tested by further observations and experiments. For example, there should be a climatic response to geomagnetic reversals or excursions ('failed reversal' events during which the geomagnetic field dips to a low value but returns with the same polarity). A relatively recent excursion was the Laschamp event, when the geomagnetic field briefly ($\lesssim$1 kyr duration) dropped to around 10% of its present strength and the GCR flux approximately doubled [Wagner *et al.*, 2000]. Based on several independent radio-isotope measurements, the Laschamp event has been precisely dated at (40.4 ± 2.0) kyr ago (2σ error) [Guillou *et al.*, 2004].

No evidence of climate change was observed in the GRIP (Greenland) ice core during the Laschamp event [Wagner *et al.*, 2001]. However several climatic effects were recorded elsewhere. A pronounced reduction of the East Asia monsoon was registered in Hulu Cave, China [Wang *et al.*, 2001]. At the same time, a brief wet period was recorded in speleothems found in tropical northeastern Brazil—a region that is presently semi-arid [Wang *et al.*, 2004]. The wet period was precisely U/Th dated to last 700 ± 400 yr from 39.6 to 38.9 kyr ago; this was the only recorded period of stalagmite growth in the 30 kyr interval from 47 to 16 kyr ago. Further evidence has recently been found in deep-sea cores from the South Atlantic, by analysing Nd isotopes as a sensitive proxy of the thermohaline ocean circulation [Piotrowski *et al.*, 2005]. A brief, sharp reduction of North Atlantic Deep Water (NADW) was recorded (i.e. towards colder conditions) coincident with the Laschamp event. In summary, there appears to be evidence for climatic responses at the time of the Laschamp event associated with the hydrological cycle.

4.5 Galactic variability

On much longer timescales, up to 1 Gyr, Shaviv (2002) has reported evidence for the occurrence of ice-age epochs on Earth during crossings of the solar system with the galactic spiral arms. The GCR flux reaching the solar system should periodically increase with each crossing of a galactic spiral arm due to the locality of the GCR sources and the subsequent 'diffusive' trapping of charged particles in the interstellar magnetic fields. This expectation is supported by the GCR exposure age recorded in iron meteorites [Shaviv, 2002].

This observation has been strengthened by Shaviv and Veizer (2003), who find a close correlation between the GCR flux and ocean temperatures reconstructed from δ^{18}O in calcite and aragonite shells found in sediments from the tropical seas (30°S–30°N), deposited during the Phanerozoic eon (the past 550 Myr, corresponding to the age of multicellular animal life on Earth) [Veizer *et al.*, 2000]. Both the GCR flux and

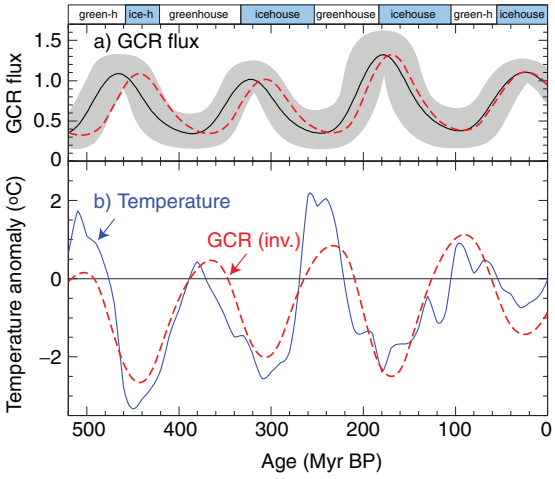

Figure 12.16. Correlation of cosmic rays and climate over the past 500 Myr [Shaviv and Veizer, 2003]: a) GCR mean flux variations as the solar system passes through the spiral arms of the Milky Way, reconstructed from iron meteorite exposure ages [Shaviv, 2002], and b) ocean temperature anomalies reconstructed from δ^{18}O in calcite shells found in sediments from the tropical seas [Veizer *et al.*, 2000]. Panel a) shows the nominal reconstructed GCR flux (solid black curve) and the error range (grey band). The dashed red curves in panels a) and b) shows the best fit of the GCR flux to the temperature data (which is given by the solid blue curve in panel b), within the allowable error (note inverted GCR scale in panel b). The data are de-trended and smoothed. The shaded blue bars at the top represent cool climate modes for Earth (icehouses) and the white bars are warm modes (greenhouses), as established from sediment analyses elsewhere.

ocean temperatures appear to follow the same periodicity of about 140 Myr and the same phase (Fig. 12.16). Extended periods of high GCR flux are found to coincide with cold epochs on Earth, when glaciation reached to low latitudes ('icehouse' climate). Conversely, during periods of low GCR flux, the climate was warm ('greenhouse'). Alternative explanations, such as increased CO_2 levels, fail to account for a 140 Myr periodicity.

5. GCR-cloud-climate Mechanisms

Mechanisms have been proposed to link the GCR flux in the atmosphere to atmospheric processes that can influence the climate. These mechanisms involve two effects of cosmic rays on the atmosphere, both involving changes in clouds. Firstly, the ionisation rate of air in the troposphere (the lowest 10–15 km of the atmosphere) varies with the cosmic ray flux. One hypothesis is that the ionisation rate influences the production of new aerosol particles in the atmosphere, and that these new particles can ultimately affect the formation of cloud droplets. Secondly, cosmic ray ionisation appears to modulate the entire ionosphere-earth electrical circuit and, in particular, the current flowing between the ionosphere and Earth. Note that, whereas solar UV influences the ionisation of the ionosphere, the current flowing between the ionosphere and Earth is determined by the tropospheric ionisation (impedance), which is unaffected by solar UV. The second hypothesis is that changes in this current influence the properties of clouds through processes involving charge effects on droplet freezing. Both mechanisms involve a number of steps between the initial effect of cosmic rays on the atmosphere and the ultimate effect on clouds and climate.

The effect of GCRs on the atmosphere is one mechanism by which solar variations can affect the climate system. Another mechanism, which has also received much attention, is the influence of variations in ultraviolet radiation on upper atmospheric ozone concentrations, and the subsequent effect of these variations on the general pattern of heating and circulation in the atmosphere (§3.1).

5.1 The importance of clouds in the climate system

Clouds account for a global average 28 Wm^{-2} net cooling of the climate system [Hartmann, 1993] so even small changes in their average coverage or their reflectivity of solar radiation can have significant effects on the climate. They absorb longwave terrestrial radiation, which leads

to a heating of Earth's surface at night, but they also reflect incoming solar shortwave radiation, leading to a cooling of the surface during the day. The net effect of clouds has been shown by models and observations to be cooling.

Layered clouds covering large areas—such as marine stratus and stratocumulus—make the greatest contribution to the cooling of the climate system, by reflection of solar radiation. Climate scientists are interested in how such clouds might respond to changes in air pollution [IPCC, 2001]. Increases in aerosol particle concentrations over the last century has led to an increase in cloud droplet concentrations in polluted regions. The net effect on cloud reflectivity is estimated to have produced a globally-averaged radiative forcing of as much as -2 Wm^{-2} since the start of the Industrial Revolution (the negative sign indicates a reduction, i.e. a cooling effect). The GCR-cloud-climate hypothesis is that long term changes in GCR flux might also have contributed to changes in cloud properties, although the effects are likely to be masked in regions where air pollution can lead to large changes in cloud properties.

Clouds also have important effects on the redistribution of energy in the climate system. In particular, release of latent heat in the mid troposphere supplies energy to the atmospheric general circulation. Processes that affect the release of latent heat have the potential to affect weather patterns and the climate more generally (e.g. [Nober *et al.*, 2003]). Ice formation is especially important in the energy budget of clouds. One hypothesis connecting GCR flux and cloud processes involves effects on ice formation at the tops of clouds.

5.2 GCRs in Earth's atmosphere

Cosmic rays comprise high energy (GeV and above) particles (mostly protons and helium nuclei) which ionise the atmosphere and produce air ions or "small ions". Away from continental sources of radon, cosmic rays dominate the production of air ions all the way to Earth's surface. The combination of two geophysical factors, geomagnetism and solar variability, modulate the ionisation rate (§3.2 and Figs. 12.3, 12.4 and 12.17). These factors, together with the cosmic ray energy spectrum, lead to a temporal and spatial distribution of cosmic rays entering the atmosphere, with about a factor 4 higher flux at the poles than at the equator. Solar magnetic activity controls the heliospheric magnetic field and modulates the cosmic ray flux, primarily below energies of about 10 GeV per nucleon. The amplitude of solar-cycle variation in ionisation rate is approximately 15% peak-to-peak, globally averaged. A long term decrease in cosmic ray flux during the last century (and starting at the

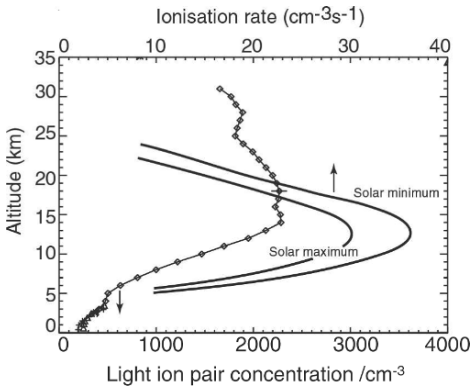

Figure 12.17. Variation with altitude of the ion-pair production rate in the atmosphere, and typical steady state ion-pair concentrations [Harrison and Carslaw, 2003]. The variation of ionisaton rate between the maximum and minimum of the 11 year solar cycle is indicated (see also Fig. 12.3).

end of the Little Ice Age; see Fig. 12.8) has also been detected, based on a number of reconstructions [Lockwood, 2003, Carslaw *et al.*, 2002].

The ion-pair production rate is balanced by processes of recombination and scavenging by aerosol particles and clouds, leading to steady state bipolar ion concentrations in the lowest part of the atmosphere of about 500 cm^{-3}, rising to a maximum of about 3000–4000 cm^{-3} at around 15 km. In the lower atmosphere the scavenging by aerosols dominates removal of ions and reduces steady state ion concentrations to typically less than one-fifth of what would occur in aerosol-free air.

5.3 Ion-induced particle formation

One mechanism for a GCR-climate interaction is that cosmic rays might influence the atmospheric concentration of cloud condensation nuclei. Cloud condensation nuclei are the aerosol particles upon which cloud droplets form, so any change in their abundance will influence the microphysical and even dynamical properties of clouds.

The continuous processes of particle removal in the atmosphere by deposition to the surface, cloud scavenging and self coagulation mean that the rate at which particles are produced influences the particle concentration at any one time. Particles are produced in the atmosphere through primary mechanisms (direct injection of new, mostly large, particles into the atmosphere, such as sea spray) or through gas-to-particle conversion (nucleation, often termed secondary particle formation). It

has been proposed that ions in the atmosphere can affect the rate of formation of particles by this latter mechanism. Unfortunately, the mechanisms of particle nucleation even in the neutral atmosphere are poorly understood [Kulmala *et al.*, 2004], making it difficult to quantify the contribution of ion-mediated processes. Despite these uncertainties, however, an increasing number of experimental and modelling studies suggest that ions can play a significant role in particle formation, at least under some conditions.

To understand the influence of ions on particle formation requires a brief introduction to the mechanism involving neutral molecules. Nucleated particles are formed in the atmosphere from condensable vapours. The range of molecules suitable for particle formation is very limited; laboratory and theoretical studies suggest that only sulphuric acid and ammonia are effective, although a range of organic species probably also contribute to growth of the new nm-sized molecular clusters. New particles consist of clusters of molecules as small as two in number. In a nucleation burst, particle concentrations at 3 nm size (the smallest size observable with commercially-available instruments) may be as high as 10^6 cm^{-3}, although concentrations of around 10^4 cm^{-3} are more typical. To be effective as cloud condensation nuclei (CCN) on which water can condense under typical atmospheric conditions requires growth of these new particles to around 40 nm diameter or more, which occurs through further condensation over several hours or days after nucleation. Cloud condensation nucleus concentrations rarely exceed a few hundred per cubic centimetre, less than one-hundredth the concentration of particles produced during nucleation. The survival rate of new particles as they grow to CCN sizes is therefore a critical parameter, and likely to be influenced by ionisation. Particle formation tends to occur readily and frequently in the upper troposphere where the condensable vapours are most supersaturated (due primarily to low ambient temperatures). In the lower atmosphere, nucleation tends to occur during 'aerosol bursts', involving long periods of no new production followed by brief (several hour) periods of rapid production.

Although only a small fraction of nucleated particles grow to CCN sizes, and only a small fraction of these are likely to have been caused by ion processes, it is worth noting that cloud reflectivity, which is important in climate change, is highly sensitive to very small changes in CCN concentration. The change in cloud reflectivity, R, approximately depends on the number of droplets, N, according to

$$\frac{\Delta R}{R} = (1 - A) \cdot \frac{\Delta N}{N}$$

Thin stratocumulus clouds that cover an appreciable fraction of the ocean typically have a reflectivity of around 0.5 and a droplet concentration of 100 cm^{-3}. For such clouds, a change of only 1% in droplet number ($\Delta N = 1$ cm^{-3}) would change the reflectivity by 0.5%.

There are two ways in which ions can increase the effective production rate of particles at readily-observable sizes of about 3 nm diameter (Fig. 12.18). They can *induce* particle formation by stabilising a cluster of condensable molecules such as sulphuric acid and ammonia through Coulomb attraction. They can also *mediate* the formation process by influencing the rate at which polar molecules subsequently condense [Nadykto and Yu, 2003, Nadykto and Yu, 2004, Laakso *et al.*, 2003]. The acceleration of cluster growth increases the fraction of particles that survive removal by coagulation before reaching observable sizes of 3 nm. Beyond about 5 nm the electrostatic effects become negligible in influencing subsequent coagulation and growth rates. However, coagulational loss rates of new particles fall dramatically beyond this size also. So with regard to the survival of particles up to CCN sizes, the critical size range is below 5 nm, and this is exactly the range for which ions have the greatest effect.

The contribution of ionisation to particle formation will be difficult to establish unambiguously because of the great variability of observed

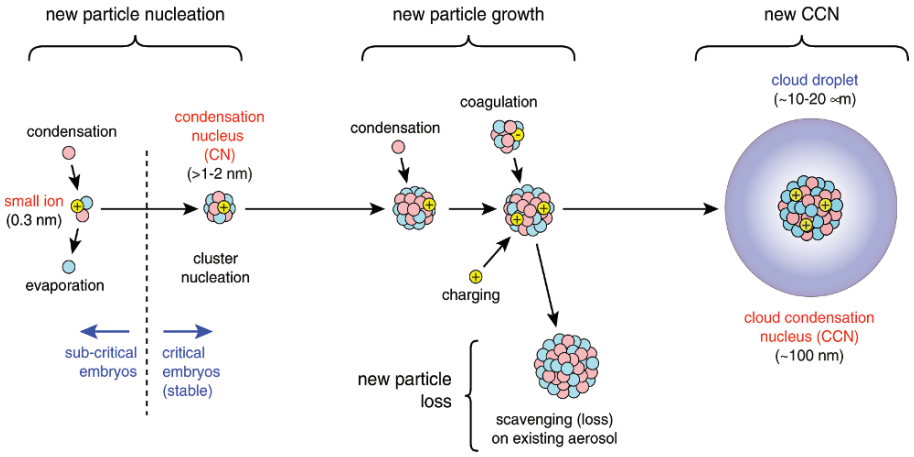

Figure 12.18. Schematic showing the nucleation and growth of new particles in the atmosphere from trace condensable vapours. Under certain conditions, the critical embryonic stage involving the nucleation and growth to sizes around 1–2 nm is enhanced by the presence of ionisation from cosmic rays. Only a small fraction of new particles reach the size of cloud condensation nuclei (CCN); most are removed by coagulation or scavenging on existing aerosol.

formation rates and because several very poorly constrained neutral mechanisms may offer alternative explanations. An upper limit to the ion-induced particle production rate close to Earth's surface (the boundary layer) is approximately 10 cm^{-3} s^{-1}, which is the maximum cosmic ray-induced ionisation rate. Observed particle production rates cover a very wide range, from as low as 0.001 to 10^4 or more cm^{-3} s^{-1} [Kulmala *et al.*, 2004], although the majority of events lie in the range 0.1-10 cm^{-3} s^{-1}. Clearly only some of the observed nucleation events can be explained in terms of ions. A further complication in assessing the potential contribution of ions to particle production rates is that particles can be observed using current instrumentation only down to 3 nm diameter, while cluster formation and growth probably begins at 0.5 nm. A large but uncertain fraction of the new clusters below 1 nm are lost through coagulation with existing particles before they grow to observable sizes [Dal Maso *et al.*, 2002].

Large positive cluster ions with atomic mass numbers up to 2500 have been detected in the upper troposphere using an aircraft-based large-ion mass spectrometer [Eichkorn *et al.*, 2002]. The charged clusters were composed of hydrogen atoms, acetone, sulphuric acid and water. The largest ions are probably very small charged aerosols formed through coagulation of neutral sulphuric acid-water clusters with charged clusters. The observations do not allow the origin of the neutral clusters to be identified, but one possible source is ion-ion recombination. These observations provide strong evidence for the ion-mediated formation and growth of aerosol particles in the upper troposphere. Cluster ions have also been observed near Earth's surface [Horrak *et al.*, 1998] in urban air, and have been shown [Yu and Turco, 2000] to be consistent with expected charged cluster growth rates.

A number of modelling studies have examined how air ions can influence the formation rate of new particles and their subsequent growth rate in different parts of the atmosphere, and have attempted to quantify how aerosol concentrations might respond to changes in ionisation rate.

The model simulations have typically used box models in which particle formation and growth is simulated under realistic atmospheric conditions for a period of several hours to days. The models include the processes of cluster formation, growth, coagulation between the clusters (an effective cluster growth mechanism) and coagulation loss of the clusters to existing, much larger, particles. The model experiments have been conducted using prescribed ionisation rates for a range of atmospheric conditions and for cases with and without charge effects. Our quantitative understanding of the kinetics and thermodynamics of neutral and charged clusters, and their interaction with larger particles and

other molecules, is currently limited. As a result, independent model simulations currently disagree regarding the regions of the atmosphere where ion-induced nucleation is likely to be important in determining the production rate of new particles.

The first simulations of ion cluster formation and growth [Yu and Turco, 1997] examined their role in aircraft exhausts. Results suggested that the number of ions produced in the exhaust was an important factor in the determining the number of particles. Later box model simulations [Yu and Turco, 2001] under normal atmospheric conditions examined how the presence of ions could enhance the formation and growth rate of sulphuric acid and water clusters. They treated particle formation as a kinetic process and adjusted the coagulation and condensation rates to take into account electrostatic forces. The model results of Yu and Turco (2001) emphasise the important effect of enhanced condensation of sulphuric acid vapour for the growth to observable sizes.

An important quantity is the fraction of ionisation events resulting in new observable particles. Yu and Turco (2001) estimate that a 25% increase in the ionisation rate would result in a 7–9% increase in the total concentration of particles between 3 and 10 nm. Thus, although every ion serves as a site for cluster formation, only approximately 1 in 3 of the new ion-induced clusters is able to grow to observable sizes of 3–10 nm. Even fewer are likely to survive to typical CCN sizes of 40 nm. Although Yu and Turco (2001) simulated particle growth out to such sizes, the results are difficult to put into context because in the real atmosphere, over several hours or days, many other processes will affect the survival of the particles than are represented in the simple box model.

Yu (2002) has also used the model to identify regions of the atmosphere where ion-mediated processes might be most important. He concluded (again, using a box model) that particle concentrations in the upper troposphere were unlikely to change significantly due to small changes in ionisation rate because particle formation is already fast there. He identified the atmospheric boundary layer as one region where changes in ionisation rate could lead to changes in particle concentration (Fig. 12.19).

A second set of model simulations and comparisons with observations has been undertaken by Laakso and co-workers [Laakso *et al.*, 2002, Laakso *et al.*, 2003, Laakso *et al.*, 2004]. They compared their model calculations of positive and negative ions and neutral clusters with observations made above a Finnish forest canopy. Interestingly, they observed an excess of negative ions in the size range 1.5–3 nm and a greater charge on 3–5 nm particles than expected simply assuming

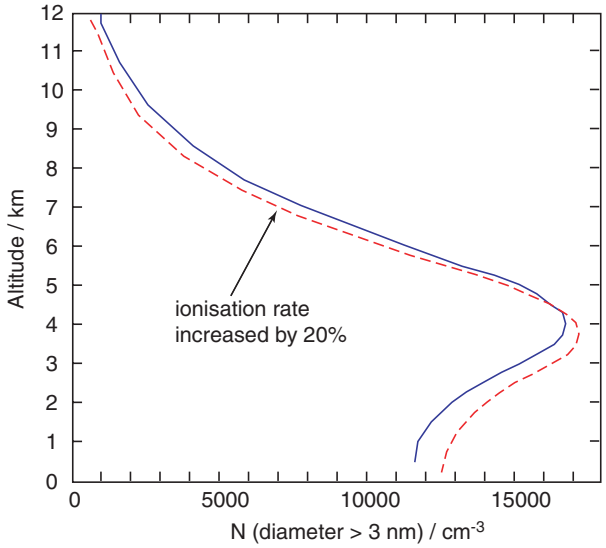

Figure 12.19. Results of a model simulation showing the effect of changes in the ionisation rate on particle concentrations resulting from sulphuric acid and water clusters [Yu, 2002]. The figure shows the concentration of particles larger than 3 nm diameter after a 3 hour simulation period. The results suggest that the greatest sensitivity is close to the Earth's surface. The model simulations assumed a realistic vertical profile of ionisation rate, increasing from 2 $cm^{-3}s^{-1}$ at the surface to 30 $cm^{-3}s^{-1}$ at 12 km. These model results differ from [Lovejoy *et al.*, 2004], who suggest that ion-induced nucleation of H_2SO_4/H_2O clusters is an efficient source of new particles in the middle and upper troposphere, but negligible in the lower troposphere.

diffusion charging equilibrium, which indicates that ions are involved in new particle formation. Overall, they conclude that ion-induced nucleation can account for some nucleation events (up to about 1 cm^{-3} s^{-1}) under conditions with low existing particle surface area, where coagulational loss of the new clusters is small.

Lee *et al.* (2003) have shown that observed ultrafine particles (<9 nm diameter) in the upper troposphere can be explained using an ion-induced mechanism [Lovejoy *et al.*, 2004]. However, high particle formation rates are also predicted assuming classical homogeneous nucleation of sulphuric acid and water under upper tropospheric conditions [Vehkamaki *et al.*, 2002]. At the low temperatures of the upper troposphere (190–230 K) homogeneous nucleation becomes very rapid and particles are formed at close to the molecular collision rate, so the upper troposphere is not a good place to test the importance of ion mechanisms. Ion-induced nucleation is likely to be distinguishable only in atmospheric regions where other mechanisms can be excluded.

Lovejoy *et al.* (2004) have performed similar modelling experiments to Laakso and Yu based on their own laboratory measurements of cluster thermodynamics, which was a major uncertainty in the previous simulations. The laboratory experiments [Froyd and Lovejoy, 2003a, Froyd and Lovejoy, 2003b] measured the thermodynamics for the binding of H_2SO_4 and H_2O in charged clusters of the form $HSO_4^-(H_2SO_4)_x(H_2O)_y$ and $H^+(H_2SO_4)_n(H_2O)_m$, which are believed to occur in the atmosphere (x, y, n and m are variable numbers of molecules attached to the cluster). The model of Lovejoy *et al.* (2004) differs from that of either Laakso *et al.* or Yu *et al.* because it treats cluster formation as a reversible process, with H_2SO_4 condensing and evaporating from the clusters as a kinetic process constrained by the thermodynamics of the clusters. In contrast, in the absence of such thermodynamic measurements, Yu and Turco (2001) treated cluster growth as an irreversible process, but reduced the growth rates to compensate for lack of evaporation by reducing the sticking rate of condensing H_2SO_4 molecules onto the clusters.

When the Lovejoy *et al.* (2004) model is applied to the atmosphere it produces quite a different result from Yu and Turco and Laakso *et al.* They find that ionisation is a significant source of new particles in the mid and upper troposphere but does not explain nucleation events close to the surface. They predict ion-induced nucleation rates for the upper troposphere of >100 cm^{-3}d^{-1} (0.001 cm^{-3}s^{-1}), which are broadly consistent with observations. One major obstacle to confirming the accuracy of the model is the sensitivity of calculated nucleation rates to the input parameters of temperature, relative humidity and H_2SO_4 gas phase concentration, with the latter being the most difficult to measure. In general, though, the Lovejoy *et al.* (2004) model can explain the limited available observed nucleation rates for temperatures below 270 K, but it under-predicts rates for the higher temperatures found closer to the surface. Closer to the surface, it is likely that other factors accelerate cluster growth, such as condensation of organic molecules.

In summary, three independent models of ion-induced particle formation have been developed based on different assumptions. Currently, all of the models suggest that ions play an important role in particle formation somewhere in the atmosphere, but the models disagree on exactly where in the atmosphere ions are likely to be most important. If ion-induced nucleation is influencing the production rate of new particles then it is reasonable to expect that CCN concentrations will respond in some way to changes in the ionisation rate. Further model simulations taking into account a wider range of realistic atmospheric processes will be needed—as well as further laboratory and field measurements—to quantify the expected CCN production rates.

5.4 The global electric circuit and effects on clouds

A second mechanism for a GCR-climate interaction concerns the influence of cosmic rays on the global electrical current flowing between the ionosphere and Earth's surface. Decadal changes in the ionospheric potential and surface potential gradient have been observed [Markson, 1981, Harrison, 2004] and explained in terms of changes in the cosmic ray flux. A number of studies have suggested that the associated change in current flowing in the fair weather part of the atmosphere may influence cloud processes.

Figure 12.20 shows the main features of the global electric circuit [Rycroft *et al.*, 2000]. Thunderstorms generate an electric current that flows to the conducting ionosphere. The ionospheric potential drives a current through the fair weather part of the atmosphere with a global mean current density of approximately 2 pA m^{-2}. A surface potential gradient of about 100 Vm^{-1} is established across a near surface resistance, where ion concentrations are low due to efficient removal of free ions to aerosol particles.

Harrison (2004) has shown that the surface potential gradient at Eskdalemuir, Scotland (55° 19', 3° 12' W) decreased by ∼25% between 1920 and 1950 and, ignoring the period 1950–1970 dominated by nuclear

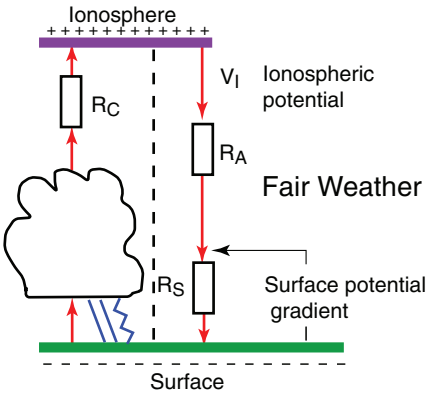

Figure 12.20. Simplified global electric circuit. Thunderstorms generate an electric current that flows through a resistance R_C to the conducting ionosphere. This establishes a positively-charged ionosphere with respect to Earth's surface. The ionospheric potential V_I drives a current through the fair weather part of the atmosphere, represented by the resistance $R_A + R_S$. A surface potential gradient of about 100 V/m is generated across the near-surface resistance, R_S. The fair weather current density is approximately 2 pA m^{-2}.

weapons tests, continued to decrease through the 1970s. Beryllium-10 concentrations in the Greenland ice core decreased by 34% over the same period, and other reconstructions suggest a decrease of around 20% [Lockwood, 2003, Carslaw *et al.*, 2002]. Figure 12.20 helps to explain how changes in cosmic rays could lead to changes in the surface potential gradient. First of all, it is worth noting that a decrease in cosmic ray flux would reduce the local ionisation rate close to the surface, resulting in an increase in electrical resistance and potential gradient there, opposite to what has been observed. So a direct local effect of cosmic rays can be excluded as an explanation for the long term changes in surface potential gradient. The positive correlation between cosmic rays and the surface potential gradient implies a control of the electric circuit in the charging part of the circuit; that is cosmic ray ionisation controls the electrical resistance between the top of thunderstorms (the current generators) and the ionosphere. Reductions in the potential gradient arise from a decrease in the current flowing in the electrical circuit, as a result of the increased resistance R_C.

The ionospheric potential has also been observed to correlate with surface cosmic ray flux over a shorter period from the 1950s to 1980s [Markson, 1981], amounting to a 10–20% variation in potential for a 10% change in surface cosmic ray flux. The response of the ionospheric potential to changes in cosmic ray flux is somewhat less than implied by the study of Harrison.

Williams (2003) has suggested that long-term decreases in aerosol pollution at the Scottish site could be an alternative explanation for the decrease in surface potential gradient. Aerosol particles reduce the conductivity of air by scavenging ions, so a long-term decrease in atmospheric particulate loading at the Scottish site would be needed to explain the decrease in potential gradient. The local evidence suggests that aerosol changes alone are unlikely to explain the long-term decrease in potential gradient observed, and that changes in cosmic rays have influenced the long-term properties of Earth's electric circuit [Harrison, 2004].

What effect might these changes in the electrical circuit have on the atmosphere? Physical mechanisms linking changes in the ionosphere-earth current to changes in the properties of clouds have been developed in a number of papers by B. Tinsley and co-workers [Tinsley, 1991, Tinsley, 1996a, Tinsley, 1996b, Tinsley, 2000, Tinsley and Deen, 1991, Tinsley *et al.*, 1989, Tinsley and Heelis, 1993, Tinsley *et al.*, 2000, Tinsley *et al.*, 2001], and recently reviewed by Carslaw *et al.* (2002) and Harrison and Carslaw (2004). The central hypothesis is that the electrical current flowing into the tops of supercooled clouds leads to relatively highly

charged cloud droplets and aerosol particles which can affect the formation of ice crystals.

The tops of many clouds exist in a supercooled state, with water droplets persisting to temperatures far below the freezing point of water. Droplet freezing between 0°C and about −37°C requires ice nuclei—a small subset of atmospheric aerosol particles able to induce ice crystallization. The formation of ice crystals in such clouds causes the release of latent heat and greatly influences the generation of precipitation since ice crystals in the presence of liquid droplets grow rapidly. The effect of cosmic rays on cloud processes is proposed to proceed through the following steps: 1) variations in cosmic rays modulate the magnitude of the ionosphere-earth current and the current flowing into clouds; 2) this increases the charges on cloud droplets and aerosol particles at cloud boundaries, which may then be entrained inside clouds; 3) changes in the charge carried by aerosol particles and cloud droplets influences the ice formation rate in clouds below 0°C; and 4) changes in cloud development, precipitation and release of latent heat result from changes in freezing rates.

Direct observation of changes in cloud properties due to changes in the ionosphere-earth current have not been made, and are unlikely to succeed in the near future due to our very poor understanding of what controls ice formation, even in the absence of weak cloud electrification. In addition, cloud properties are highly variable, being driven mostly by large scale meteorological effects, so any cosmic ray modulation of their properties will be masked. Confirmation of the Tinsley hypothesis therefore relies on observing and explaining statistical relationships between atmospheric variables and cosmic ray flux, and a number of such attempts have been made by Tinsley and co-workers.

The proposed mechanism linking cosmic rays, atmospheric electrical current and cloud droplet freezing is plausible. Both theory and observation support the build-up of space charge at the top and bottom of clouds (regions of net unipolar charge carried by ions, aerosol and droplets; see Fig. 12.21). Space charge is created because cloud particles efficiently scavenge small ions, thereby reducing the local conductivity, and leading to an increased local potential gradient through the cloud to drive a constant current density. Observed space charge densities can be as high as $100e$ cm^{-3} at cloud upper and lower surfaces [Harrison and Carslaw, 2003]. Although not yet confirmed by observations, the magnitude of space charge is likely to be modulated by the ionosphere-earth current density flowing into cloud tops.

The mechanism therefore hinges upon an enhanced freezing probability of supercooled droplets in the elevated space charge environment.

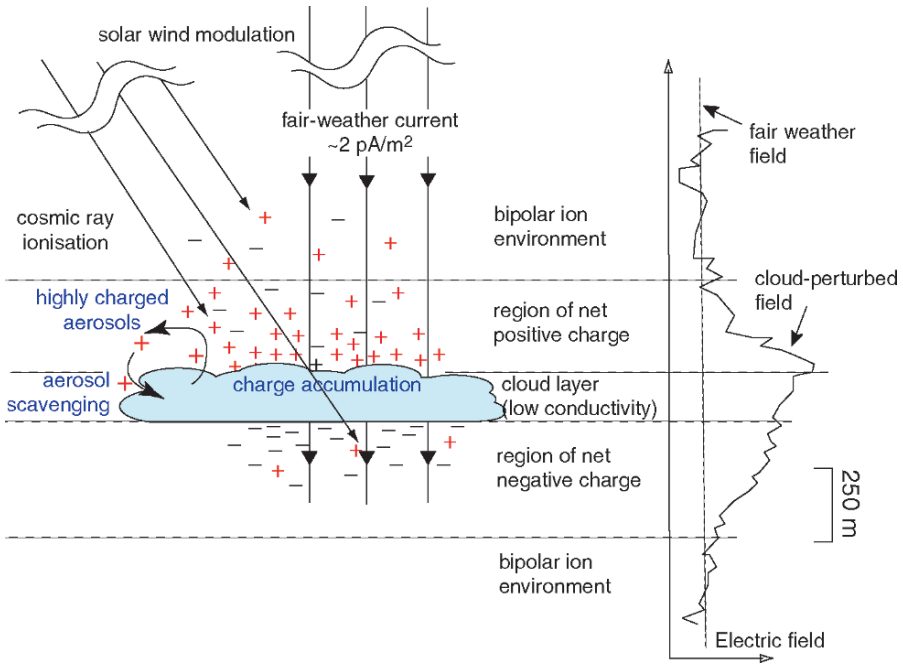

Figure 12.21. Schematic showing the creation of space charge at the top and bottom of clouds. This space charge can become attached to droplets and aerosol particles, and then entrained within clouds.

Charge carried by droplets themselves does not affect the droplet freezing probability. The more likely possibility is that charged aerosol particles (some of which will be ice nuclei) will be scavenged by droplets more rapidly than their uncharged counterparts [Tinsley *et al.*, 2000, Tripathi and Harrison, 2002]. This so-called *contact* ice nucleation, involving the scavenging of an aerosol particle by a supercooled droplet, is one of several mechanisms that can lead to freezing (the others involve ice-forming nuclei already within the droplet). Observations have allowed simple parameterisations of the number of such contact nuclei to be fitted in terms of the supersaturation of the vapour with respect to ice [Meyers *et al.*, 1992], although field observations of ice formation rates and of ice nuclei themselves show great variability. Tripathi and Harrison (2002) estimated, for a droplet of radius 26 μm, that a particle charge of $10e$ would be comparable to a change in ice nucleus concentration expected from a 1 K reduction in temperature. Thus, any effect of changes in space charge on ice formation in cloud tops are likely to be very small for changes in the ionosphere-earth current of a few per cent.

In summary, changes in the global electric circuit over decadal periods have been observed and attributed to changes in the cosmic ray flux, although there is uncertainty regarding alternative explanations. Changes in the surface potential gradient and ionospheric potential imply a change in the fair weather electric current. The current flowing into cloud tops may influence the production of ice crystals, although any effect is likely to be small compared with the very large and poorly understood variability in ice formation rates. It is certainly not contentious to state that changes in ice formation would affect the release of latent heat, precipitation, general atmospheric dynamics and climate. However, the coupling of changes in Earth's electric circuit and atmospheric dynamics involves small estimated forcings that are likely to be difficult to observe in the real atmosphere.

6. Conclusions and Future Prospects

During the last few years, a wide range of new palaeoclimatic evidence has shown that solar/GCR forcing has exerted a major influence on past climate. Although this evidence is largely based on correlations between cosmic ray- and climate archives—which do not necessarily imply a casual connection—the sheer diversity and quality of the correlations preclude mere chance association.

However, although the evidence for solar/GCR forcing of climate appears beyond doubt, the mechanism remains unclear. There are only two candidates for the forcing agent: a) the solar irradiance, or a spectral component such as the UV, or b) galactic cosmic rays, which are modulated by the solar wind. In the former case, GCR variability is considered to be a proxy for changes of solar irradiance or UV, which are assumed to vary hand-in-hand with long-term changes of solar magnetic activity. Although secular changes of solar magnetic activity are well established, its link with changes of irradiance and UV is not; beyond the 11-yr sunspot cycle, there is no direct or indirect evidence (from sun-like stars) that there are secular variations of the Sun's irradiance on timescales shorter than about 10 Myr. This does not rule them out, of course, but it does illustrate how little is understood at present of the solar forcing mechanism.

An influence of GCRs on climate can in principle be unambiguously resolved from a direct solar irradiance/UV effect since the former implies that climate will also be affected by variations of the geomagnetic field or, on a longer time scale, of the galactic environment. Indeed, some evidence has been reported of both such associations. However, at this

stage, the data are insufficient either to confirm or to rule out either candidate as the forcing agent.

Satellite cloud observations over the last 20 years may have provided an important clue on the climate mechanism: low cloud amount appears to be modulated by the solar cycle. If confirmed by further observations, this would be climatically significant since clouds exert a strong control on Earth's radiative energy balance. Present low cloud data favour an association with GCR intensity, although they are also consistent with irradiance/UV variations (but with the opposite sign; increased low clouds are associated with increased GCRs but *decreased* irradiance/UV).

Theoretical and modelling studies suggest that cosmic rays may influence cloud microphysics in several ways. These include ion-induced nucleation of new aerosols from trace condensable vapours, and the formation of relatively highly charged aerosols and cloud droplets at cloud boundaries, which may enhance the formation of ice particles, thereby releasing latent heat and affecting precipitation. Recent observations support the presence of ion-induced nucleation in the atmosphere, although its significance in the presence of other sources of variability is not yet established.

The key to further progress on the cosmic ray-cloud-climate question is to understand the physical mechanism. This requires an experimental study of the fundamental microphysical interactions between cosmic rays and clouds. Demonstrating overall cause and effect in the atmosphere beginning with changes in ionisation rate and ending with observations of perturbed clouds will be quite challenging. For this reason an experiment is under construction by a multi-disciplinary team [CLOUD collaboration] to study GCR-cloud microphysics under carefully controlled conditions in the laboratory using a CERN particle beam as an artificial source that closely simulates natural cosmic rays [CLOUD proposal, 2000, 2004, Kirkby, 2002]. The apparatus includes an advanced cloud chamber and reactor chamber where the atmosphere is realistically represented by moist air charged with aerosol and trace gases. The chambers are equipped with a wide range of external instrumentation to monitor and analyse their contents. The thermodynamic conditions anywhere in the troposphere and stratosphere can be re-created within the chambers. In contrast with experiments in the atmosphere, CLOUD can compare processes when the cosmic ray beam is present and when it is not, and all experimental parameters can be controlled.

With the expected advances in experiments, observations and theory in the next few years, there are good prospects that we may finally be able to answer William Herschel's two-centuries-old question of why the price of wheat in England was lower when there were many sunspots.

References

Beer, J., (2000), Long-term indirect indices of solar variability, *Space Sci. Rev.* **94**, 53–66.

Bond, G.C., and R. Lotti (1997a), Iceberg discharges into the North Atlantic on millennial time scales during the last glaciation, *Science* **267**, 1005–1010.

Bond, G.C., W. Showers, M. Cheseby, R. Lotti, P. Almasi, P. deMenocal, P. Priore, H. Cullen, I. Hajdas and G. Bonani (1997b), A pervasive millennial-scale cycle in North Atlantic Holocene and glacial climates, *Science* **278**, 1257–1266.

Bond, G.C., B. Kromer, J. Beer, R. Muscheler, M.N. Evans, W. Showers, S. Hoffmann, R. Lotti-Bond, I. Hajdas and G. Bonani (2001), Persistent solar influence on North Atlantic climate during the Holocene, *Science* **294**, 2130–2136.

Carslaw, K.S., R.G. Harrison and J. Kirkby (2002), Cosmic rays, clouds, and climate, *Science* **298**, 1732–1737.

Channell, J.E.T., D.A. Hodell, J. McManus and B. Lehman (1998), Orbital modulation of the Earth's magnetic field intensity, *Nature* **394**, 464–468.

Christl, M., C. Strobl and A. Mangini (2003), Beryllium-10 in deep-sea sediments: a tracer for the Earth's field intensity during the last 200,000 years, *Quat. Sc. Rev.* **22**, 725–739.

Christl, M., A. Mangini, S. Holzkämper, C. Spötl (2004), Evidence for a link between the flux of galactic cosmic rays and Earth's climate during the past 200,000 years, *J. Atm. Sol. Terr. Phys.* **66**, 313–322.

CLOUD proposal (CLOUD collaboration, 2000–06), A study of the link between cosmic rays and clouds with a cloud chamber at the CERN PS, CERN-SPSC-2000-021, SPSC-P-317; CERN-SPSC-2000-030, SPSC-P-317-Add-1; CERN-SPSC-2000-041, SPSC-P-317-Add-2; SPSC-M-721, CERN-SPSC-2004-023. `http://www.cern.ch/cloud/iaci_workshop/cloud.html`

CLOUD collaboration: *Univ. Aarhus*, Denmark; *Univ. Bergen*, Norway; *California Institute of Technology*, USA; *CERN*, Switzerland; *Danish National Space Center*, Denmark; *Finnish Meteorological Institute*, Finland; *Univ. Helsinki*, Finland; *Univ. Kuopio*, Finland; *Lebedev Physical Institute*, Russia; *Univ. Leeds*, UK; *Univ. Mainz*, Germany; *Max-Planck Institute for Nuclear Physics - Heidelberg*, Germany; *Univ. Missouri-Rolla*, USA; *Paul Scherrer Institute*, Switzerland; *State University of New York at Albany*, USA; *Univ. Reading*, UK; *Rutherford Appleton Laboratory*, UK; *Tampere University of Technology*, Finland; and *Univ. Vienna*, Austria.

Dal Maso, M., M. Kulmala, K.E.J. Lehtinen, J.M. Makela, P. Aalto and C.D. O'Dowd (2002), Condensation and coagulation sinks and formation of nucleation mode particles in coastal and boreal forest boundary layers, *J. Geophys. Res.-Atmos.*, **107**, art. no.-8097.

Eddy, J.A., (1976), The Maunder minimum, *Science* **192**, 1189.

Eichkorn, S., S. Wilhelm, H. Aufmhoff, K.H. Wohlfrom, and F. Arnold (2002), Cosmic ray-induced aerosol formation: First observational evidence from aircraft-based ion mass spectrometer measurements in the upper troposphere, *Geophys. Res. Lett.* **29**, 43.

Foukal, P., G. North, T. Wigley (2004), A stellar view on solar variations and climate, *Science* **306** (2004) 68.

Fröhlich, C. (2000), Observations of irradiance variability, *Space Science Reviews* **94**, 15–24.

Froyd, K.D., and E.R. Lovejoy (2003a), Experimental thermodynamics of cluster ions composed of H_2SO_4 and H_2O. 1. Positive ions, *J. Phys. Chem. A*, **107**, 9800–9811.

Froyd, K.D., and E.R. Lovejoy (2003b), Experimental thermodynamics of cluster ions composed of H_2SO_4 and H_2O. 2. Measurements and *ab initio* structures of negative ions, *J. Phys. Chem. A*, **107**, 9812–9824.

Gallup, C.D., H. Cheng, F.W. Taylor and R.L. Edwards, Direct determination of the timing of sea level change during Termination II, *Science* **295**, 310–313 (2002).

Ganopolski, A. and S. Rahmstorf (2001), Rapid changes of glacial climate simulated in a coupled climate model, *Nature* **409**, 153–158.

Gleeson, L.J., and W.I. Axford (1967), Cosmic rays in the interplanetary medium, *Astrophys. Journal* **149**, 1115–1118.

Guillou, H., B.S. Singer, C. Laj, C. Kissel, S. Scaillet and B.R. Jicha (2004), On the age of the Laschamp geomagnetic excursion, *Earth and Planet. Sci. Lett.* **227**, 331–343.

Haigh, J.D., (1996), The impact of solar variability on climate, *Science* **272**, 981.

Harrison, R.G., and K.S. Carslaw (2003), Ion-aerosol-cloud processes in the lower atmosphere, *Rev. Geophys.,* **41**, art. no.-1012.

Harrison, R.G., (2004), Long-range correlations in measurements of the global atmospheric electric circuit, *J. Atmos. Sol.-Terr. Phys.*, **66**, 1127–1133.

Hartmann, D.L., Radiative effects of clouds on Earth's climate, in *Aerosol-Cloud-Climate Interactions*, International Geophysics Series **54**, ed. P.V. Hobbs, Academic Press Inc., San Diego (1993), 151–173.

Henderson, G.M., and N.C. Slowey (2000), Evidence from U/Th dating against Northern Hemisphere forcing of the penultimate deglaciation, *Nature* **404**, 61–66.

Herschel, W., (1801), *Philosophical Transactions of the Royal Society*, **91**, 265–283.

Horrak, U., A. Mirme, J. Salm, E. Tamm and H. Tammet (1998), Air ion measurements as a source of information about atmospheric aerosols, *Atmos. Res.*, **46**, 233–242.

Hu, F.S., D. Kaufman, S. Yoneji, D. Nelson, A. Shemesh, Y. Huang, J. Tian, G.C. Bond, B. Clegg and T. Brown (2003), Cyclic variation and solar forcing of Holocene climate in the Alaskan sub-Arctic, *Science* **301**, 1890–1893.

Huang, S., H.N. Pollack and P.-Y. Shen (2000), Temperature trends over the past five centuries reconstructed from borehole temperatures, *Nature* **403**, 756-758.

IPCC Third Assessment Report, *Climate Change 2001: The Scientific Basis*, Intergovernmental Panel on Climate Change, eds. J.T. Houghton *et al.*, Cambridge University Press, UK.

Kernthaler, S.C., R. Toumi and J.D. Haigh (1999), *Geophys. Res. Lett.* **26**, 863; T.B. Jorgensen and A.W. Hansen (2000), *J. Atm. Sol. Terr. Phys.* **62**, 73; J.E. Kristjánsson and J. Kristiansen (2000), *J. Geophys. Res.* **105**, 11851; J.E. Kristjánsson, A. Staple and J. Kristiansen (2002), *Geophys. Res. Lett.* **29**, 10.1029/2002GL015646; B. Sun and R.S. Bradley (2002), *J. Geophys. Res.* **107**, D14, 10.1029/2001-JD000560.

Kirkby, J. (2002), CLOUD: a particle beam facility to investigate the influence of cosmic rays on clouds, *CERN-EP-2002-019* and *Proc. of the Workshop on Ion-Aerosol-Cloud Interactions* (2001), ed. J. Kirkby, CERN, Geneva, *CERN 2001-007*, 175–248. `http://cloud.web.cern.ch/cloud/iaci_workshop/proceedings.html`

Kirkby, J., A. Mangini and R.A. Muller (2004), The glacial cycles and cosmic rays, *CERN-PH-EP-2004-027*. `http://arxiv.org/abs/physics/0407005`

Klein, J., J.C. Lerman, P.E. Damon and T. Linick (1980), Radiocarbon concentrations in the atmosphere: 8000 year record of variations in tree rings, *Radiocarbon* **22**, 950–961.

Knie, K., G. Korschinek, T. Faestermann, E.A. Dorfi, G. Rugel and A. Wallner (2004), ^{60}Fe anomaly in a deep-sea manganese crust and implications for a nearby supernova source, *Phys. Rev. Lett.* **93**, 171103.

Kulmala, M., H. Vehkamaki, T. Petajda, M. Dal Maso, A. Lauri, V.M. Kerminen, W. Birmili and P.H. McMurry (2004), Formation and growth rates of ultrafine atmospheric particles: a review of observations, *J. Aerosol. Sci.*, **35**, 143–176.

Laakso, L., J.M. Mäkelä, L. Pirjola and M. Kulmala (2002), Model studies on ion-induced nucleation in the atmosphere, *J. Geophys. Res.* D20, 10.1029/2002JD002140.

Laakso, L., M. Kulmala and K.E.J. Lehtinen (2003), Effect of condensation rate enhancement factor on 3-nm (diameter) particle formation in binary ion-induced and homogeneous nucleation, *J. Geophys. Res.-Atmos.*, **108**, art. no.-4574.

Laakso, L., T. Anttila, K.E.J. Lehtinen, P.P. Aalto, M. Kulmala, U. Horrak, J. Paatero, M. Hanke and F. Arnold (2004), Kinetic nucleation and ions in boreal forest particle formation events, *Atmos. Chem. Phys.*, **4**, 2353-2366.

Larkin, A., J.D. Haigh and S. Djavidnia (2000), The effect of solar UV irradiance variations on the Earth's atmosphere, in *Solar Variability and Climate*, eds. E. Friis-Christensen *et al.*, *Space Science Reviews* **94**, Nos. 1–2, 145–152.

Lean, J.L., J. Beer, R. Bradley (1995), Reconstruction of solar irradiance since 1610: Implications for climatic change, *Geophys. Res. Lett.* **22** (1995) 3195-3198.

Lean, J.L., Y.-M. Wang and N.R. Sheeley (2002), The effect of increasing solar activity on the Sun's total and open magnetic flux during multiple cycles: Implications for solar forcing of climate, *Geophys. Res. Lett.* **29**, 2224.

Lee, S.H., J.M. Reeves, J.C. Wilson, D.E. Hunton, A.A. Viggiano, T.M. Miller, J.O. Ballenthin and L.R. Lait (2003), Particle formation by ion nucleation in the upper troposphere and lower stratosphere, *Science*, **301**, 1886–1889.

Lockwood, M., R. Stamper and M.N. Wild (1999), A doubling of the Sun's coronal magnetic field during the past 100 years, *Nature* **399**, 437.

Lockwood, M., (2003), Twenty-three cycles of changing open solar magnetic flux, *J. Geophys. Res-Space Phys.*, **108**, art. no.-1128.

Lovejoy, E.R., J. Curtius and K.D. Froyd (2004), Atmospheric ion-induced nucleation of sulphuric acid and water, *J. Geophys. Res.* **109**, D08204, doi:10.1029/2003JD004460.

Mann, M.E., R.S. Bradley and M.K. Hughes (1998), Global-scale temperature patterns and climate forcing over the past six centuries, *Nature* **392**, 779–787.

Mann, M.E., R.S. Bradley and M.K. Hughes (1999), Northern Hemisphere temperatures during the past millennium: inferences, uncertainties, and limitations, *Geophys. Res. Lett.* **26**, 759–762.

Markson, R., (1981), Modulation of the Earth's electric-field by cosmic-radiation, *Nature*, **291**, 304–308.

Marsh, N., and H. Svensmark (2003), Galactic cosmic ray and El Niño-Southern Oscillation trends in International Satellite Cloud Climatology Project D2 low-cloud properties, *J. Geophys. Res.* **108** D6, 4195.

Meyers, M.P., P.J. Demott and W.R. Cotton (1992), New primary ice-nucleation parameterisations in an explicit cloud model, *J. Appl. Meteorol.*, **31**, 708–721.

McIntyre, S., and R. McKitrick (2005), Hockey sticks, principal components and spurious significance, *Geophys. Res. Lett.*, doi: 2004GL012750.

Moberg, A, D.M. Sonechkin, K. Holmgren, N.M. Datsenko and W. Karlén, (2005), Highly variable Northern Hemisphere temperatures reconstructed from low- and high-resolution proxy data, *Nature* **433**, 613—618.

Muller, R.A., and G.J. MacDonald (1997), Glacial cycles and astronomical forcing, *Science* **277**, 215–218.

Muller, R.A., and G.J. MacDonald (2000), *Ice Ages and Astronomical Causes*, Springer Praxis, Chichester, UK.

Nadykto, A.B., and F.Q. Yu (2003), Uptake of neutral polar vapour molecules by charged clusters/particles: Enhancement due to dipole-charge interaction, *J. Geophys. Res.-Atmos.*, **108**, art. no.-4717.

Nadykto, A.B., and F.Q. Yu (2004), Dipole moment of condensing monomers: A new parameter controlling the ion-induced nucleation, *Phys. Rev. Lett.*, **93**, art. no.-016101.

Neff, U., *et al.* (2001), Strong coincidence between solar variability and the monsoon in Oman between 9 and 6 kyr ago, *Nature* **411**, 290–293.

Nober, F.J., H.F. Graf and D. Rosenfeld (2003), Sensitivity of the global circulation to the suppression of precipitation by anthropogenic aerosols, *Glob. Planet. Change*, **37**, 57–80.

Parker, E.N., (1965), The passage of energetic charged particles through interplanetary space, *Planet. Space Sc.* **13**, 9–49.

Piotrowski, A.M., S.L. Goldstein, S.R. Hemming and R.G. Fairbanks (2005), Temporal relationships of carbon cycling and ocean circulation at glacial boundaries, *Science* **307**, 1933–1938.

Pollack, H.N., and J.E. Smerdon (2004), Borehole climate reconstructions: spatial structure and hemispheric averages, *J. Geophys. Res.* **109**, doi:10.1029/2003JD004163.

Raisbeck, G.M., F. Yiou, J. Jouzel and J.-R. Petit (1990), ^{10}Be and ^{2}H in polar ice cores as a probe of the solar variability's influence on climate, *Phil. Trans. Roy. S. Lond.* **A300**, 463–470.

Reid, G.C. (1987), Influence of solar variability on global sea surface temperatures, *Nature* **329**, 142–143.

Rossow, W.B., A.W. Walker, D.E. Beuschel, and M.D. Roiter (1996), International Satellite Cloud Climatology Project (ISCCP): documentation of new cloud datasets, WMO/TD **737**, World Meteorological Organization, Geneva.

Rycroft, M.J., S. Israelsson and C. Price (2000), The global atmospheric electric circuit, solar activity and climate change, *J. Atm. Sol. Terr. Phys.* **62**, 1563-1576.

Shaviv, N.J., (2002), Cosmic ray diffusion from the galactic spiral arms, iron meteorites, and a possible climatic connection, *Phys. Rev. Lett.* **89**, 051102.

Shaviv, N.J., and J. Veizer (2003), Celestial driver of Phanerozoic climate?, *GSA Today*, Geological Society of America, July 2003, 4–10.

Shindell, D. *et al.* (1999), Solar cycle variability, ozone, and climate, *Science* **284**, 305–308.

Spötl, C., A. Mangini, N. Frank, R.,Eichstädter and S.J. Burns (2002), Start of the last interglacial period at 135 ka: Evidence from a high Alpine speleothem, *Geology* **30**, no. 9, 815–818.

St-Onge, G., J.S. Stoner, C. Hillaire-Marcel (2003), Holocene palaeomagnetic records from the St. Lawrence Estuary, eastern Canada: centennial- to millennial-scale geomagnetic modulation of cosmogenic isotopes, *Earth and Planet. Sci. Lett.* **209**, 113–130.

Svensmark, H., and E. Friis-Christensen (1997), Variation in cosmic ray flux and global cloud coverage—a missing link in solar-climate relationships, *J. Atm. Sol. Terr. Phys.* **59**, 1225.

Tinsley, B.A., G.M. Brown and P.H. Scherrer (1989), Solar variability influences on weather and climate - possible connections through cosmic-ray fluxes and storm intensification, *J. Geophys. Res.-Atmos.*, **94**, 14783–14792.

Tinsley, B.A., (1991), Interpretation of short-term solar variability effects in the troposphere, *J. Geomagn. Geoelectr.*, **43**, 775–783.

Tinsley, B.A., and G.W. Deen (1991), Apparent tropospheric response to MeV-GeV particle-flux variations - a connection via electrofreezing of supercooled water in high-level clouds, *J. Geophys. Res.-Atmos.* **96**, 22283–22296.

Tinsley, B.A., and R.A. Heelis (1993), Correlations of atmospheric dynamics with solar-activity evidence for a connection via the solar-wind, atmospheric electricity, and cloud microphysics, *J. Geophys. Res.-Atmos.*, **98**, 10375–10384.

Tinsley, B.A., (1996a), Correlations of atmospheric dynamics with solar wind-induced changes of air-earth current density into cloud tops, *J. Geophys. Res.-Atmos.*, **101**, 29701–29714.

Tinsley, B.A., (1996b), Solar wind modulation of the global electric circuit and apparent effects on cloud microphysics, latent heat release, and tropospheric dynamics, *J. Geomagn. Geoelectr.*, **48**, 165–175.

Tinsley, B.A., (2000), Influence of solar wind on the global electric circuit, and inferred effects on cloud microphysics, temperature, and dynamics in the troposphere, *Space Sci. Rev.*, **94**, 231–258.

Tinsley, B.A., R.P. Rohrbaugh, M. Hei and K.V. Beard (2000), Effects of image charges on the scavenging of aerosol particles by cloud droplets and on droplet charging and possible ice nucleation processes, *Atmos. Res.* **57**, 2118–2134.

Tinsley, B.A., R.P. Rohrbaugh and M. Hei (2001), Electroscavenging in clouds with broad droplet size distributions and weak electrification, *Atmos. Res.* **59**, 115–135.

Tripathi, S.N., and R.G. Harrison (2002), Enhancement of contact nucleation by scavenging of charged aerosol particles, *Atmos. Res.* **62**, 57–70.

Usoskin, I.G., K. Mursula, S.K. Solanki, M. Schüssler and G.A. Kovaltsov (2002), A physical reconstruction of cosmic ray intensity since 1610, *J. Geophys. Res.* **107**, doi:10.1029/2002JA009343.

Usoskin, I.G., N. Marsh, G.A. Kovaltsov, K. Mursula and O.G. Gladysheva (2004), Latitudinal dependence of low cloud amount on cosmic ray induced ionisation, *Geophys. Res. Lett.*, doi: 10.1029/2004GL019507.

Vehkamaki, H., M. Kulmala, I. Napari, K.E.J. Lehtinen, C. Timmreck, M. Noppel and A. Laaksonen (2002), An improved parameterization for sulfuric acid-water nucleation rates for tropospheric and stratospheric conditions, *J. Geophys. Res.-Atmos.*, **107**, art. no.-4622.

Veizer, J., Y. Godderis and L.M. François (2000), Evidence for decoupling of atmospheric CO_2 and global climate during the Phanerozoic eon, *Nature* **408**, 698–701.

Visser, K., R. Thunell and L. Stott (2003), Magnitude and timing of temperature change in the Indo-Pacific warm pool during deglaciation, *Nature* **421**, 152–155.

Wagner, G., D M. Livingstone, J. Masarik, R. Muscheler and J. Beer (2001), Some results relevant to the discussion of a possible link between cosmic rays and the Earth's climate, *J. Geophys. Res.* **106**, D4, 3381–3387.

Wagner, G., J. Masarik, J. Beer, S. Baumgartner, D. Imboden, P.W. Kubik, H.-A. Synal and M. Suter (2000), Reconstruction of the geomagnetic field between 20 and 60 kyr BP from cosmogenic radionuclides in the GRIP ice core, *Nuc. Inst. Meth. Phys. Res.* **B172**, 597–604.

Wang, Y.J., H. Cheng, R.L. Edwards, Z.S. An, J.Y. Wu, C.-C. Shen, J.A. Doral (2001), A high-resolution absolute-dated late Pleistocene monsoon record from Hulu Cave, China, *Science* **294**, 2345–2348.

Wang, X., A.S. Auler, R.L. Edwards, H. Cheng, P.S. Cristalli, P.L. Smart, D.A. Richards and C.-C. Shen (2004), Wet periods in northeastern Brazil over the past 210 kyr linked to distant climate anomalies, *Nature* **432**, 740–743.

White, W.B., J. Lean, D.R. Cayan and M.D. Dettinger (1997), Response of global upper ocean temperature to changing solar irradiance, *J. Geophys. Res.* **102**, C2, 3255–3266.

White, W.B., D.R. Cayan and J. Lean (1998), Global upper ocean heat storage response to radiative forcing from changing solar irradiance and increasing greenhouse gas/aerosol concentrations, *J. Geophys. Res.* **103**, C10, 21333–21366.

Williams, E.R., (2003), Comment to "Twentieth century secular decrease in the atmospheric potential gradient" by Giles Harrison, *Geophys. Res. Lett.* **30**, art. no.-1803.

Winograd, I.J., T.B. Coplen, J.M. Landwehr, A.C. Riggs, K.R. Ludwig, B.J. Szabo, P.T. Kolesar, and K.M. Revesz (1992), Continuous 500,000-year climate record from vein calcite in Devils Hole, Nevada, *Science* **258**, 255–260.

Yamazaki, T., and H. Oda (2002), Orbital influence on Earth's magnetic field: 100,000-year periodicity in inclination, *Science* **295**, 2435–2438.

Yu, F.Q., and R.P. Turco (1997), The role of ions in the formation and evolution of particles in aircraft plumes, *Geophys. Res. Lett.* **24**, 1927–1930.

Yu, F.Q., and R.P. Turco (2000), Ultrafine aerosol formation via ion-mediated nucleation, *Geophys. Res. Lett.* **27**, 883-886.

Yu, F., and R.P. Turco (2001), From molecular clusters to nanoparticles: The role of ambient ionisation in tropospheric aerosol formation, *J. Geophys. Res.* **106**, 4797–4814.

Yu, F.Q., (2002), Altitude variations of cosmic ray induced production of aerosols: Implications for global cloudiness and climate, *J. Geophys. Res.-Space Phys.*, **107**, art. no.-1118.